BCG-based vaccines with two doses of 80 mg in monkeys was sufficient to induce the desired virus-specific cell-mediated immune responses, thus presenting the possibility of using the vaccine candidates orally in humans (Kawabara *et al.*, 2002).

These studies also demonstrated that the proposed prime-boost regimen was safe to use in the non-human primate hosts: no detectable adverse effects resulted from vaccination in any of the immunized monkeys. One of the concerns regarding the use of recombinant BCG in Thailand was possible side effects or reduced efficiency in people who were previously immunized with BCG. A series of animal experiments were conducted to address these issues. We showed that prior immunization with BCG did not affect the induction of HIV p24 antigen-specific DTH (delayed-type hypersensitivity) in guinea pigs that were immunized with the recombinant BCG-based HIV vaccines. However, previous exposure to BCG vaccination in monkeys did seem to reduce Gag-specific cellular immune responses in the immunized monkeys by about 50%.

We believe that the recombinant BCG-based HIV vaccines would be safe to use in Thailand. To date, more than two billion people worldwide have been vaccinated with BCG against TB with a proven safety record. With regard to the use of the recombinant vaccinia virus-based HIV vaccines, we believe that the non-replicative DIs strain presents a safer alternative to the MVA (modified vaccinia Ankara) that is being widely used in HIV-1 vaccine development elsewhere. Like the MVA-based HIV-1 vaccines, the recombinant non-replicative vaccinia virus DIs is capable of efficiently expressing the HIV-1 antigens in mammalian host cells. However, the DIs-based viruses lack the replicative ability in these cells, thus producing no infectious viruses. In contrast, MVA is able to replicate in mammalian cells like BHK and CV-1 following infection (Carroll and Moss, 1997). The structural basis for this distinction between the DIs virus and MVA is not yet known. It was shown that the DIs virus as a smallpox vaccine failed to induce a skin reaction in inoculated infants and permitted revaccination by another smallpox vaccine strain without complications, demonstrating a safety advantage over the use of MVA as a recombinant vaccinia vector (Fujii and Minamitani, 1968).

In order to assure the safety of the T-J CAVRP candidate vaccines, the pilot products of these vaccines are evaluated in baby monkeys, as well as in adult monkeys. Studies showed that as much as 800 mg of the recombinant BCG-based HIV vaccines by oral administration, or repeated subcutaneous injections of 50 mg of the vaccine, did not cause any detectable adverse effects when compared directly with the standard BCG vaccine (Sukpanichnant *et al.*, Department of Pathology, Faculty of Medicine, Siriraj Hospital, Mahidol University, December 2003, unpublished data). Similar safety experiments are underway to evaluate the recombinant non-replicative vaccinia DIs-based HIV vaccines.

FUTURE PLANS

The above-mentioned first generation candidate vaccine incorporates the *gag* gene only, and does not induce sterile immunity because the immunized monkeys do not suppress primary viremia completely after the SHIV challenge. The *gag* gene product cannot induce neutralizing antibodies that block virus entry. Therefore, introduction of the *env* gene to current constructs may be important to enable the vaccines to prevent both HIV-1 infection and disease progression. Furthermore, the construct of a single *gag* gene would have a restricted range of CTL responder population in which the HLA type is involved. To address these issues, future research may be conducted to improve the capacity and expression level of incorporated HIV-1 *env* genes in rBCG and rDIs.

To improve immunogenicity of the vaccine constructs, antigen expression in BCG or in DIs should be optimized. Regarding rBCG, we have already found that the codon-optimized *gag* p24 gene is expressed at a drastically higher level than the native *gag*; this strategy can be applied to other rBCG constructs to make them more immunogenic (Kanekiyo *et al.*, unpublished data). Such investigations are continuing now through collaboration between Japan and Thailand. These approaches are of particular importance to obtain an HIV vaccine that is highly effective.

ACKNOWLEDGEMENTS. We would like to thank Drs. Bonnie Mathieson, Jorge Flores and Rebecca Sheets, Division of AIDS, National Institute of Allergy and Infectious Diseases (NIAID), National Institutes of Health (NIH), Bethesda, MD, USA; Dr. Bernard Moss, Laboratory of Viral Diseases, NIAID, for his helpful discussions; and Drs. Hidemi Takahashi, and Yohko Nakagawa, Department of Microbiology and Immunology, Nippon Medical School, Tokyo, for their helpful discussions. Japan Science Technology Incorporation, the Organization of Pharmaceutical Safety and Research, the "Panel on AIDS" of the US-Japan Cooperative Medical Science Program, the Human Science Foundation of Japan, and the Japanese Ministry of Health, Labor and Welfare also supported this work. This study was also supported by the AIDS vaccine project in conjunction with the Japan Science and Technology Cooperation.

REFERENCES

Albright, A.V., Shieh, J.T., Itoh, T., Lee, B., Pleasure, D., O'Connor, M.J., Doms, R.W., and Gonzalez-Scarano, F. (1999). Microglia express CCR5, CXCR4, and CCR3, but of these, CCR5 is the principal coreceptor for human immunodeficiency virus type 1 dementia isolates. *J. Virol.* 73:205–213.

Ananworanich, J., Nuesch, R., Teeratakulpisarn, S., Srasuebkul, P., Chuenyam, T., Siangphoe, U., Ungsedhaphand, C., Phanuphak, P., and Ruxrungtham, K. (2003). In vivo cell-mediated immunity in subjects with undetectable viral load on protease inhibitor-based versus non-protease inhibitor-based highly active antiretroviral therapy. *J. Acquir. Immune. Defic. Syndr.* 32:570–572.

Ariyoshi, K., Promadej, N., Ruxrungtham, K., and Sutthent, R. (2002). Toward improved evaluation of cytotoxic T-lymphocyte (CTL)-inducing HIV vaccines in Thailand. *AIDS Res. Hum. Retroviruses* 18:737–739.

Balachandra, K., Matsuo, K., Sutthent, R., Hoisanka, N., Boonsarthorn, N., Sawanpanyalert, P., Warachit, P., Yamazaki, S., and Honda, M. (2002). Characteristic of HIV-1 in V3 loop region based on serореactivity and amino acid sequences in Thailand. *Asian Pac. J. Allergy Immunol.* 20: 93–98.

Carroll, M.W. and Moss, B. (1997). Host range and cytopathogenicity of the highly attenuated MVA strain of vaccinia virus: propagation and generation of recombinant viruses in a nonhuman mammalian cell line. *Virology* 238:198–211.

Chujoh, Y., Matsuo, K., Yoshizaki, H., Nakasatomi, T., Someya, K., Okamoto, Y., Nagamawa, S., Haga, S., Yoshikura, H., Yamazaki, A., Yamazaki, S., and Honda, M. (2002). Cross-clade neutralizing antibody production against human immunodeficiency virus type 1 clade E and B' strains by recombinant *Mycobacterium bovis* BCG-based candidate vaccine. *Vaccine* 20: 797–804.

Fujii, R., and Minamitani, M. (1968). Virus infections with exanthema. *Saishin Igaku* 23:1146–1155. In Japanese.

Fukada, K., Tomiyama, H., Wasi, C., Matsuda, T., Kusagawa, S., Sato, H., Oka, S., Takebe, Y., and Takiguchi, M. (2002). Cytotoxic T-cell recognition of HIV-1 cross-clade and clade-specific epitopes in HIV-1-infected Thai and Japanese patients. *AIDS* 16:701–711.

Hamano, T., Sawanpanyalert, P., Yanai, H., Piyaworawong, S., Hara, T., Sapsutthipas, S., Phromjai, J., Yamazaki, S., Yamamoto, N., Warachit, P., Honda, M., and Matsuo, K. (2004). Determination of HIV-1 CRF01_AE gag p17 and env-V3 consensus sequences for HIV/AIDS vaccine design. *AIDS Res. Hum. Retroviruses*, in press.

Ishii, K., Ueda, Y., Matsuo, K., Matsuura, Y., Kitamura, T., Kato, K., Izumi, Y., Someya, K., Ohsu, T., Honda, M., and Miyamura, T. (2002). Structural analysis and application of vaccinia virus DIs strain as a completely replication-deficient viral vector for HIV vaccine. *Virology* 302:433–444.

Izumi, Y., Ami, Y., Matsuo, K., Someya, K., Sata, T., Yamamoto, N., and Honda, M. (2003). Intravenous inoculation of replication-deficient recombinant vaccinia virus DIs expressing simian immunodeficiency virus gag controls highly pathogenic simian-human immunodeficiency virus in monkeys. *J. Virol.* 77:13248–13256.

Kanekiyo, M., Matsuo, K., Hamatake, M., Yamamoto, N., Honda, M. (2003). Optimization of codon usage confers vigorous expression in recombinant Mycobacterium bovis BCG vaccine. Proceedings of the International Symposium on Research and Development of Recombinant BCG and Vaccinia Virus-based HIV Vaccine. Tokyo, Japan: 21–24.

Kawahara, M., Hashimoto, A., Toida, I., and Honda, M. (2002). Oral recombinant *Mycobacterium bovis* bacillus Calmette-Guerin expressing HIV-1 antigens as a freeze-dried vaccine induces long-term, HIV-specific mucosal and systemic immunity. *Clin. Immunol.* 105:326–331.

Kitamura, T., Kitamura, Y., and Tagaya, I. (1967). Immunogenicity of an attenuated strain of vaccinia virus on rabbits and monkeys. *Nature* 215:1187–1188.

Kitsutani, P. T., Naganawa, S., Shiino, T., Matsuda, M., Honda, M., Yamada, K., Taki, M., and Sugiura, W. (1998). HIV type 1 subtypes of nonhemophiliac patients in Japan. *AIDS Res. Hum. Retroviruses* 14:1099–1103.

Kusagawa, S., Sato, H., Tomita, Y., Tatsumi, M., Kato, K., Motomura, K., Yang, R., and Takebe, Y. (2002). Isolation and characterization of replication-competent molecular DNA clones of HIV type 1 CRF01_AE with different coreceptor usages. *AIDS Res. Hum. Retroviruses* 18:115–122.

Lagranderie, M., Balazuc, A.M., Gicquel, B., and Gheorghiu, M. (1997). Oral immunization with recombinant *Mycobacterium bovis* BCG simian immunodeficiency virus nef induces local and systemic cytotoxic T-lymphocyte responses in mice. *J. Virol.* 71: 2303–2309.

Matsuo, K., Nakasone, T., Izumi, Y., Ami, Y., Ohsu, T., Hamano, T., Yamamoto, N., Yamazaki, S., and Honda, M. (2002). SIV Gag-expressing recombinant BCG-prime and recombinant vaccinia virus DIs strain-boost regimen evokes protective immune response in monkey. XIV International AIDS Conference; July 2002. Barcelona, Spain. ThOrA1222.

Nabel, G.J. (2001). Challenges and opportunities for development of an AIDS vaccine. *Nature* 410:1002–1007.

Naganawa, S., Na Ayuttaya, P.L, Duangchanda, S., Auwanit, W., Warachit, P., Miyamura, K., Yamazaki, S., and Honda, M. (1997). A characteristic change of consensus core motif in the V3 region of HIV type 1 clade B, but not in clade E, in Thailand. *AIDS Res. Hum. Retroviruses* 13:271–273.

Ogura, A., Noguchi, Y., Yamamoto, Y., Shibata, S., Asano, T., Okamoto, Y., and Honda, M. (1996). Localization of HIV-1 in human thymic implant in SCID-hu mice after intravenous inoculation. *Int. J. Exp. Pathol.* 77:201–206.

Okamoto, Y., Ogura, A., Shibata, S., Amagai, T., Katsura, Y., Asano, T., and Honda, M. (1997). Simple i.v. inoculation of HIV-1 to Thy/Liv SCID-hu mice induce reproducible HIV infection with narrowing of medulla in human thymic implant. *J. Vet. Med. Sci.* 59:259–263.

Okamoto, Y., Eda, Y., Ogura, A., Shibata, S., Amagai, T., Katsura, Y., Asano, T., Kimachi, K., Makizumi, K., and Honda, M. (1998). In SCID-hu mice, passive transfer of a humanized antibody prevents infection and atrophic change of medulla in human thymic implant due to intravenous inoculation of primary HIV-1 isolate. *J. Immunol.* 160:69–76.

Pintanodhai, N., Kangwanshiratada, O., and Charoenwongse, P. (2003). Serological analysis of human leukocyte antigens-A and -B antigens in Thai patients with nasopharyngeal carcinoma. *J. Med. Assoc. Thai.* 86 Suppl 2:S237–S241.

Ruxrungtham, K., and Phanuphak, P. (2001). Update on HIV/AIDS in Thailand. *J. Med. Assoc. Thai.* 84 Suppl 1:S1–S17.

Ruxrungtham, K., Buranapraditkul, S., Kosoonsiriluk, S., Kerdsanti, S., Hansasutha, P., Sirivichaykul, S., Rowland-Jones, S., and Phanuphak, P. (2003). HIV-1 specific cytotoxic T-lymphocytes (CTLs) study. Proceedings of the International Symposium on Research and Development of Recombinant BCG and Vaccinia Virus-based HIV Vaccine. Tokyo, Japan: 43–52.

Sakai, K., Shinohara, K., Takahashi, E., Izumi, Y., Ami, Y., Sasaki, Y., Nakasone, T., and Honda, M. (2001). Molecular cloning of a pathogenic simian-human immunodeficiency virus for HIV/AIDS monkey model. Sixth International Congress on AIDS in Asia and the Pacific; 2001 Oct 5–10. Melbourne, Australia. Abstract p. 84. *Proc. Int. Cong. AIDS Asia Pacific* 6:84.

Schultz, A.M., and Bradac, J.A. (2001). The HIV vaccine pipeline, from preclinical to phase III. *AIDS* 15: 8147–8158.

Shinohara, K., Sakai, K., Ando, S., Ami, Y., Yoshino, N., Takahashi, E., Someya, K., Suzaki, Y., Nakasone, T., Sasaki, Y., Kaizu, M., Lu, Y., and Honda, M. (1999). A highly pathogenic simian/human immunodeficiency virus with genetic changes in cynomolgus monkey. *J. Gen. Virol.* 80:1231–1240.

Sutthent, R., Sumrangsurp, K., Wirachsilp, P., Chaisilwattana, P., Roongpisuthipong, A., Chaiyakul, P., Noona, P., Honda, M., and Warachit, P. (2001). Diversity of HIV-1 subtype E in semen and cervicovaginal secretion. *J. Hum. Virol.* 4:260–268.

Tagaya, I., Kitamura, T., and Sano, Y. (1961). A new mutant of dermovaccinia virus. *Nature* 192: 381–382.

Vejbaesya, S., Eiermann, T.H., Suthipinitharm, P., Bancha, C., Stephens, H.A., Luangtrakool, K., and Chandanayingyong, D. (1998). Serological and molecular analysis of HLA class I and II alleles in Thai patients with psoriasis vulgaris. *Tissue Antigens* 52:389–392.

Ward, F.E., Tuan, S., and Haynes, B.F. (1995). Analysis of HLA Frequencies in Population Cohorts for Design of HLA-Based HIV Vaccines. In: Korber, B., Brander, C., Walker, B.D., Koup, R., Moore, J.P., Haynes, B.F., and Myers, G. (eds.), *HIV Molecular Immunology Database 1995*, Theoretical Biology and Biophysics Group, Los Alamos National Laboratory, Los Alamos, NM. pp. IV-10–16.

Weniger, B.G., Takebe, Y., Ou, C.Y., and Yamazaki, S. (1994). The molecular epidemiology of HIV in Asia. *AIDS* 8 Suppl 2:S13–S28.

P1: FQF
KI055-Lu & Essex ISBN 0306484838 March 16, 2004 10:2

AIDS RESEARCH AND HUMAN RETROVIRUSES
Volume 20, Number 3, 2004, pp. 000–000

Sequence Note

Determination of HIV Type 1 CRF01_AE gag p17 and env-V3 Consensus Sequences for HIV/AIDS Vaccine Design

TAKAICHI HAMANO,[1] PATHOM SAWANPANYALERT,[2] HIDEKI YANAI,[1,3] SURACHAI PIYAWORAWONG,[4] TAKASHI HARA,[5] SOMPONG SAPSUTTHIPAS,[1] JURAIRAT PHROMJAI,[2] SHUDO YAMAZAKI,[1,5] NAOKI YAMAMOTO,[5] PAIJIT WARACHIT,[6] MITSUO HONDA,[1,5] and KAZUHIRO MATSUO[1,5]

ABSTRACT

A molecular epidemiological study of the gag p17 and env-V3 regions on HIV-infected drug users and blood donors was carried out in northern Thailand from 1998 through 2002 to determine the predominant subtype and consensus sequence (CS) for circulating HIV-1 strains. CRF01_AE was concluded to be a predominant strain and the nucleotide CSs in gag p17 and env-V3 showed only 1.26% and no difference from CS in the Los Alamos database, respectively. Our env-V3 CS was identical to the previously published CSs, suggesting that the CS was very conserved from 1990 through 2002 in Thailand. Gag p17 and env-V3 nucleotide sequences of seroconvertors in our subjects were quite similar to the CS and conserved for at least 9 and 6 years postinfection, respectively. These results suggest that the CS approach to the HIV-1 antigen design could overcome HIV diversity and help us develop an effective HIV/AIDS vaccine.

THE ANTIGEN GENES IN THE FIRST-GENERATION HIV/AIDS CANDIDATE VACCINES were obtained from isolated viruses. However, the range of amino acid (AA) changes of each isolate demonstrated more than 30% difference from the CRF01_AE consensus envelope sequence.[1] Considering the diversity of each circulating virus, investigators find it very difficult to select an optimal antigen from numerous isolates to develop an efficacious preventive HIV/AIDS vaccine. Currently, three computational methods (consensus, ancestral, and center of the tree) are being considered as a strategy for a novel antigen design of an HIV/AIDS vaccine to overcome HIV diversity.[1,2] However, these novel types of antigen have never been used for vaccine construction to control the HIV-1 CRF01_AE epidemic in Thailand. From 1998 to 2002, to characterize currently circulating viruses in northern Thailand, we determined HIV-1 subtypes among HIV-1-seropositive drug users (DUs) and blood donors (BDs) in Chiang Rai in northern Thailand using provirus sequences of gag p17 and env-V3 regions. Furthermore, CSs of both regions were classified and compared with those in the database,[3] in 1990s isolated samples[4] and in seroconvertors,[5] respectively.

One hundred and nineteen HIV-1-infected DUs and 96 BDs were investigated. Their $CD4^+$ and $CD8^+$ T lymphocyte absolute count indicated a mean value of 308/μl (range: 8–1449/μl) and 747/μl (range: 98–3079/μl) in DU, respectively. Phylogenetic tree analysis of the gag p17 and env-V3 regions revealed that the predominant HIV-1 subtype was CRF01_AE with 88% and 97% in the DU and BD groups, respectively (data not shown). Other minor subtypes were classified as B′ (Thailand variant of subtype B) and B in the both groups.

CSs of the CRF01_AE gag p17 (CSg) and env-V3 (CSe) regions were determined using proviral sequences derived from

[1]JST AIDS Vaccine Project, c/o National Institute of Health, Ministry of Public Health, Nonthaburi 11000, Thailand.
[2] National Institute of Health, Ministry of Public Health, Nonthaburi 11000, Thailand.
[3]TB/HIV Research Project, RIT-JATA, Muang District, Chiang Rai 57000, Thailand.
[4]Mae Chan Hospital, Mae Chan district, Chiang Rai 57110, Thailand.
[5]National Institute of Infectious Diseases, Japan, Tokyo 162-8640, Japan.
[6]Ministry of Public Health, Thailand, Nonthaburi 11000, Thailand.

35 and 126 individuals, respectively. These CSs were compared to the available CRF01_AE CS (CSD) in the database (Table 1).[3] In the gag p17 region, nucleotide sequence and AA alignment difference showed means of 2.66 and 5.11% from our CSg, respectively. CSg showed a difference of 1.26% in nucleotides and 3.79% in AA, as compared with CSD.[3] The average magnitude ($n = 16$) of the gag p17 nucleotide and AA difference between CSg and each isolate in Table 1 showed no significant difference from circulating viruses in our specimens (Student's t test). Furthermore, CSg and CSD of gag p17 were close to the isolates prior to 1993 than to those after 1994.

In the case of the env-V3 region, the mean differences of our nucleotide and AA sequences from CSe were 5.55 and 11.59%, respectively. The CSe of nucleotide and AA sequences were

TABLE 1. COMPARISON OF OUR CONSENSUS SEQUENCES WITH DATABASE OF HIV-1 CRF01_AE gag P17 AND env-V3[a]

	Compared to our CS of gag p17		*Compared to our CS of env-V3*	
Sample name	*Different nuc (%)*	*Different AA (%)*	*Different nuc (%)*	*Different AA(%)*
93TH057	4.55	9.85	7.62	14.29
93TH065	2.27	5.30	0.95	2.86
95TH253	3.03	6.06	12.38	37.14
93TH902	4.29	8.33	7.62	8.57
94TH702	3.03	6.06	No data	No data
94TH7091	3.03	6.06	No data	No data
95TNIH022	3.79	6.82	20.95	42.86
95TNIH047	3.79	7.58	16.19	31.43
97TH6-107	3.54	6.06	0.95	0.00
CM235	1.26	2.27	2.86	5.71
CM238	1.77	4.55	0.95	2.86
CM239	No data	No data	0.95	2.86
CM240	2.27	5.30	2.86	5.71
CM241	No data	No data	0.00	0.00
CM242	No data	No data	0.95	2.86
CM243	1.01	1.52	5.71	14.29
CM244	No data	No data	0.00	0.00
TN240	1.52	3.79	No data	No data
TN245	2.02	3.03	No data	No data
92TH022	1.01	2.27	0.95	2.86
CS from database[3]	1.26	3.79	0.00	0.00
CS from McCutchan *et al.*[4]	No data	No data	0.00	0.00
CS from Subbarao *et al.*[5]	No data	No data	0.00	0.00
Calculated by above samples				
Mean ($n = 16$)	2.64	5.30	5.12	10.89
Range	1.01–4.55	1.52–9.85	0–20.95	0–42.86
Calculated by our samples				
Mean (n = gag p17, env-V3 = 35,126)	2.66	5.11	5.55	11.59
Range	0.76–4.80	2.27–9.73	0–15.24	0–40.00
Calculated by seroconvertors' samples[5]				
Mean ($n = 102$)	No data	No data	3.14[b]	6.49[b]
Range	No data	No data	0–11.43	0–22.86
Years after seroconversion in our samples				
<1: Mean (n = gag p17, env-V3 = 9, 13)	3.17	4.80	4.91	9.67
Range	1.52–5.05	1.52–6.82	0.95–7.62	2.83—17.14
1–3: Mean (n = gag p17, env-V3 = 0, 12)	No sample	No sample	5.16	9.29
Range			1.90–0.48	2.86–17.14
3–6: Mean (n = gag p17, env-V3 = 9, 21)	2.40	4.58	5.62	12.24
Range	0.76–4.13	2.27–7.03	0.95–15.24	2.86–31.43
>6–9: Mean (n = gag p17, env-V3 = 9, 12)	2.81	6.05	7.70[c]	17.38[d]
Range	1.52–4.29	3.03–9.73	1.90–14.29	2.86–31.43

[a]CS, consensus sequence; nuc, nucleotide; AA, amino acid; SD, standard deviation.
[b]Significantly different from our samples ($p < 0.0001$).
[c,d]Significantly different from <1 sample ($p = 0.038$ and 0.010).

identical to those of CSD. The average distance ($n = 16$) of the env-V3 nucleotide and AA sequence of each isolate in the database[3] from CSe was 5.12 and 10.89%, respectively, and they showed no significant differences from circulating viruses in our specimens. CSs of nucleotide and AA of env-V3 in seroconvertors[5] who were infected during 1995–1998 were also identical to CSe. However, there was an average of 3.14% in nucleotide and 6.49% in AA differences that were significantly closer to CSe than to other available sequences. Furthermore, the CS of env-V3 that was determined by six specimens (CM235–CM244) isolated in 1990 in northern Thailand[4] was identical to CSe. 93TH065[6] and 92TH022[7] isolated from early seroconvertors indicated high similarity to CSs in both regions.

From our investigation, it was revealed that the consensus nucleotide and AA sequences of env-V3 in circulating CRF01_AE were very conserved from 1990 through 2002 in Thailand[4,5,7–9] and that the nucleotide sequence distance in the C2–V3 region from seroconvertors in DU was low[5] and each isolate was more similar to the env-V3 CS than our isolates. In addition, seven of 102 samples in DU seroconvertors in Bangkok[5] and two of six CM series samples[4] showed quite high homogeneity to CSe. In our subjects, 27 of 35 in gag p17 and 58 of 126 in env-V3 had definitive risk for HIV-1 infection from the data of Sawanpanyalert *et al.*[10–12] and were divided into four groups by year after seroconversion (less than 1 year, 1–3 years, 3–6 years, and >6–9 years). Using nucleotide and AA sequences in both regions, we compared seroconvertors (less than 1 year) with other year groups and with seroconvertors in a Bangkok DU cohort[5] as an env-V3 control. The sequence differences in gag p17 and env-V3 were not statistically significant among all year groups or the Bangkok DU group except for the >6–9 years group, which showed significant difference ($p = 0.038$ in nucleotide and 0.010 in AA levels), suggesting that seroconvertors possessed a quite similar sequence and maintained the similarity for at least 6 years. These results suggest that the CRF01_AE sequence was conserved for quite a long time and a certain specific type of virus whose sequence is close to the CS might be the one that is mainly transmitted. Furthermore, taking account of the high homogeneity of our CSs to the early isolates during the pandemic in Thailand (93TH065, 92TH022, and CM series), CRF01_AE has not been evolving in a unique direction but at random and then consequently conserves its CSs, as compared to the sequence of isolates in the pandemic stage.

As for another subtype, the env and gag AA sequences in HIV-1 subtype C isolates shared identity 92–95% and 90.5–98.7% with the South African CS, respectively.[13] Subtype C gag p17 and p24 AAs were relatively conserved and showed less than 10% diversity to CS in Botzwana.[14] Abidjan AA CS of gag p24 was 99.32% identical to reference CRF02_AG.[15] The 4 incidence and 19 prevalence cases were 97.1 and 96.6% homologous to Abidjan CS, respectively, and the range in incidence cases was narrower than that in prevalence cases.[15] These results suggest that the CS could provide a less distant virus sequence in the population than each circulating isolate even in the different subtypes.

In summary, a consensus approach for antigen genes could minimize the sequence distance from each circulating isolate and may provide an effective strategy to construct an HIV/AIDS vaccine candidate that could induce broad protective efficacy against diverse HIV-1 isolates.

ACCESSION NUMBERS

gag p17: AB115505–AB115540; env-V3: AB115782–AB115907.

ACKNOWLEDGMENTS

We gratefully acknowledge the dedicated field work of Ms. Saiyud Moolphate, Ms. Pompimon Saksoong, and other members of the TB/HIV Research Project, the RIT-JATA, the Regional Medical Sciences Centre in Chiang Rai, and the Mae Chan Hospital. We also thank Dr. Kruavon Balachandra for her kind technical support and advice. This investigation was cosponsored by grants from the Sasakawa Memorial Health Foundation, the Japanese Foundation for AIDS Prevention, and the Japan Health Sciences Foundation.

REFERENCES

1. Gaschen B, Taylor J, Yusim K, *et al.*: Diversity considerations in HIV-1 vaccine selection. Science 2002;296:2354–2360.
2. Nickle DC, Jensen MA, Gottlieb GS, *et al.*: Consensus and ancestral state HIV vaccines. Science 2003;299:1515–1518.
3. Korber B, Brander C, Haynes BF, et al. (eds.): *HIV Immunology and Sequence Databases.* Los Alamos National Laboratory, Los Alamos, NM, 2003.
4. McCutchan FE, Hegerich PA, Brennan TP, *et al.*: Genetic variants of HIV-1 in Thailand. AIDS Res Hum Retroviruses 1992;8: 1887–1895.
5. Subbarao S, Vanichseni S, Hu DJ, *et al.*: Genetic characterization of incident HIV type 1 subtype E and B strains from a prospective cohort of injecting drug users in Bangkok, Thailand. AIDS Res Hum Retroviruses 2000;16:699–707.
6. Anderson JP, Rodrigo AG, Learn GH, *et al.*: Testing the hypothesis of a recombinant origin of human immunodeficiency virus type 1 subtype E. J Virol 2000;74:10752–10765.
7. WHO Network for HIV Isolation and Characterization: HIV type 1 variation in World Health Organization-sponsored vaccine evaluation sites: Genetic screening, sequence analysis, and preliminary biological characterization of selected viral strains. AIDS Res Hum Retroviruses 1994;10:1327–1343.
8. Kalish ML, Baldwin A, Raktham S, *et al.*: The evolving molecular epidemiology of HIV-1 envelope subtypes in injecting drug users in Bangkok, Thailand: Implications for HIV vaccine trials. AIDS 1995;9:851–857.
9. Tian H, Lan C, and Chen YH: Sequence variation and consensus sequence of V3 loop on HIV-1 gp120. Immunol Lett 2002;83: 231–233.
10. Sawanpanyalert P, Supawitkul S, Yanai H, Saksoong P, and Piyaworawong S: Trend of HIV infection rates among drug users in an HIV epicenter in northern Thailand (1989–1997). J Epidemiol 1999;9:114–120.
11. Jittiwutikarn J, Sawanpanyalert P, Rangsiveroj N, and Satitvipawee F: HIV incidence rates among drug users in northern Thailand, 1993–7. Epidemiol Infect 2000;125:153–158.

12. Sawanpanyalert P, Yanai H, Kitsuwannakul S, and Nelson KE: An estimate of the number of human immunodeficiency virus (HIV)-positive blood donations by HIV-seronegative donors in a northern Thailand HIV epicenter. J Infect Dis 1996;174:870–873.
13. Williamson C, Morris L, Maughan MF, *et al.*: Characterization and selection of HIV-1 subtype C isolates for use in vaccine development. AIDS Res Hum Retroviruses 2003;19:133–144.
14. Novitsky V, Smith UR, Gilbert P, *et al.*: Human immunodeficiency virus type 1 subtype C molecular phylogeny: Consensus sequence for an AIDS vaccine design? J Virol 2002;76:5435–5451.
15. Ellenberger DL, Li B, Lupo LD, *et al.*: Generation of a consensus sequence from prevalent and incident HIV-1 infections in West Africa to guide AIDS vaccine development. Virology 2002;302:155–163.

Address reprint requests to:
Takaichi Hamano
JST AIDS Vaccine Project
c/o National Institute of Health
Ministry of Public Health
88/7 Soi Bamrasnaradura
Tivanond Road
Nonthaburi 11000, Thailand

E-mail: taka0627@yahoo.co.jp
or hamano@dmsc.moph.go.th

Prompt tumor formation and maintenance of constitutive NF-κB activity of multiple myeloma cells in NOD/SCID/γc^{null} mice

Md. Zahidunnabi Dewan,[1,7] Mariko Watanabe,[2,7] Kazuo Terashima,[1] Mizuho Aoki,[1] Tetsutaro Sata,[3] Mitsuo Honda,[4] Mamoru Ito,[5] Shoji Yamaoka,[1] Toshiki Watanabe,[6,8] Ryouichi Horie[2,8] and Naoki Yamamoto[1,4,8]

[1]Department of Molecular Virology, Bio-Response, Graduate School, Tokyo Medical and Dental University, 1-5-45 Yushima, Bunkyo-ku, Tokyo 113-8519; [2]Department of Internal Medicine, School of Medicine, Kitasato University, 1-15-1 Sagamihara, Kanagawa 228-8555; [3]Department of Pathology and [4]AIDS Research Center, National Institute of Infectious Diseases, 1-23-1 Toyama, Shinjuku-ku, Tokyo 162-8640; [5]Central Institute for Experimental Animals, 1430, Nogawa, Miyamae-ku, Kawasaki, Kanagawa 216-0001; and [6]Division of Pathology, Department of Cancer Biology Institute of Medical Science, The University of Tokyo, 4-6-1 Shirokanedai, Minato-ku, Tokyo 108-8639

(Received March 1, 2004/Revised April 28, 2004/Accepted May 10, 2004)

Clinically and biologically relevant animal models are indispensable to evaluate both the pathophysiology and strategies for diagnosis and treatment of multiple myeloma (MM). We examined the tumorigenicity of MM cell lines KMM-1 and U-266 in an *in vivo* cell proliferation model using NOD/SCID/γc^{null} (NOG) mice. Two cell lines were inoculated either subcutaneously (s.c.) in the post-auricular region or intravenously (i.v.) in the tail of NOG mice. The KMM-1 cell line produced a progressively growing large tumor with infiltration of the cells expressing human λ-chain in various organs of all NOG mice, while the U-266 cell line failed to do so. Tumor cells grown in NOG mice maintained the original histomorphology, as well as expression patterns of tumor markers human λ Ig light chain and VEGF. Tumor progression in mice also correlated with elevation of serum human soluble IL-6R and gp130. Tumor cells sustained a strong NF-κB activity *in vivo* and induced NF-κB components were indistinguishable from those in cells cultured *in vitro*. The rapid and efficient engraftment of the MM cell line in NOG mice suggests that this is a very useful animal model which could provide a novel system in which to clarify the mechanism of growth of cancer cells, as well as to develop new therapeutic regimens against MM. (Cancer Sci 2004; 95: 564–568)

Multiple myeloma (MM) is a B-cell neoplasm characterized by clonal expansion of plasma cells in the bone marrow, and is associated with neoangiogenesis and often with severe bone disease.[1–4] MM has a poor prognosis and a very short survival time, mainly because of poor efficacy of conventional and transplantation therapy. To develop novel therapies and to study the pathophysiology, a good animal model of this disease is needed. Such a model would require high engraftment efficiency and conservation of relevant tumor features.

Severe combined immunodeficiency (SCID) mice have been utilized in studies on the mechanism of MM and on therapeutic strategy.[5–10] However, this model has five major drawbacks, i.e., that tumor formation requires a long period of time, repeated transplantation, total body irradiation, and human fetal bone and anti-gp130 mAbs. Depending on the type of treatment, immunosuppressive conditioning releases a cascade of pro-inflammatory cytokines,[11] which strongly influence the activities of various cell types of tumor stroma, such as fibroblasts, myoepithelial cells, and macrophages, that are in close functional interaction with adjacent tumor cells.[12–14] Therefore, such treatments could lead to changes in relevant histomorphologic or functional features of tumors implanted into respective recipients. Furthermore, immunosuppressive pretreatment, such as irradiation, alters the expression patterns of adhesion molecules in peripheral tissues.[11] This may influence immune cell migration into such sites, causing difficulties in the interpretation of cellular transfer studies in such models.[11] In the present study, we have used a newly developed SCID mouse strain, the NOD/SCID/γc^{null} (NOG) mouse, in order to overcome such problems. This is a unique type of animal, lacking both T- and B-cells and having defects in NK activity, macrophage function, complement activity, and dendritic cell function.[15,16] MM cell lines were inoculated either subcutaneously (s.c.) in the post-auricular region or intravenously (i.v.) in the tail of NOG mice enabling both macroscopic and microscopic observation of the mechanism of tumorigenesis and malignant growth of MM.

We show here that a progressively growing large tumor was rapidly and reproducibly induced in all mice inoculated with cells of the MM cell line within only 2 to 3 weeks, and infiltration of the tumor cells was observed in various organs of NOG mice. Tumor cells sustained a strong NF-κB activity *in vivo*, which might play an important role in the cell proliferation of MM. These results suggest that the NOG mouse model of MM should be useful for investigating the *in vivo* molecular pathogenesis, infiltration into different organs, and therapeutic measures for MM patients.

Materials and Methods

Mice and cell lines. NOG mice were obtained from the Central Institute for Experimental Animals (Kawasaki, Japan). All mice were maintained under specific-pathogen-free conditions in the Animal Center of National Institute of Infectious Diseases (Tokyo). The Ethical Review Committee of the Institute approved the experimental protocol.

KMM-1 and U-266 cell lines (both of which produce λ chain), established from MM patients, and a T-cell line, Jurkat, were cultured in RPMI-1640 medium (Nikken Bio-laboratory, Kyoto, Japan) with 10% heat-inactivated fetal bovine serum (FBS; JRH Biosciences, Lenexa, KS), 2 m*M* L-glutamine, 100 U of penicillin per milliliter, and 100 μg of streptomycin per milliliter at 37°C and 5% CO_2.

Inoculation of cell lines into NOG mice. Cells were washed twice with serum-free RPMI-1640 medium. These cells were re-suspended in serum-free RPMI-1640 medium. Mice were anesthetized with ether and cells were inoculated either i.v. in the tail or s.c. in the post-auricular region of NOG mice at a dose of 2×10^6 to 10×10^6 cells per mouse.

Growth measurement of s.c. tumor and histological and immunological examination. Mice were sacrificed 40 or 60 days after in-

[7]Both authors contributed equally to this study.

[8]To whom correspondence should be addressed.
E-mail: yamamoto.mmb@tmd.ac.jp rhorie@med.kitasato-u.ac.jp
tnabe@ims.u-tokyo.ac.jp

oculation with a cell line. We measured the length, width, and height of the tumor according to the Somers scale. Blood was collected from the heart of mice with heparinized syringes. Peripheral blood mononuclear cells (PBMNCs) were isolated from the blood by density gradient concentration with Ficoll-Hypaque. Cytospin specimens of PBMNCs were prepared and fixed in methyl alcohol for May-Grunwald and Giemsa staining. Tumor tissues and various organs were fixed with Streck Tissue Fixative (S.T.F) and processed to paraffin wax-embedded sections for staining with hematoxylin and eosin (H&E) and immunostaining. Paraffinized cryosections of tumors and various organs were deparaffinized and hydrated in xylenes or clearing agents and graded alcohol series, and then rinsed for 5 min in water. Deparaffinized samples were incubated with 0.025% trypsin/phosphate-buffered saline (PBS) for 30 min followed by washing, and then incubated with 0.3% methanol for 30 min at room temperature and washed twice with PBS. Immunostaining was done as described in the Vector M.O.M. immunodetection kit (Cat.# PK-2200, Vector Laboratories, Inc., Burlingame, CA) for MM cells with a 1:500 dilution of primary mouse monoclonal antibody specific for human λ Ig light chain (M614, Dako) and rabbit polyclonal antibody specific for VEGF (A-20, Santa Cruz Biotechnology, Santa Cruz, CA). This was followed by washing in PBS and then incubation with a secondary antibody, M.O.M. biotinylated anti-mouse and anti-rabbit IgG. The sections were washed in PBS and further incubated with VECTASTAIN *Elite* ABC for 20 min at room temperature. Positive staining was visualized after incubation of these samples with a mixture of 0.05% 3,3'-diaminobenzidine tetrahydrochloride in 50 m*M* Tris-HCl buffer and 0.01% hydrogen peroxide for 5 min. The samples were counterstained with hematoxylin for 2 min, hydrated completely, cleaned in xylene and then mounted.

Measurement of serum human soluble IL-6 (sIL-6), sIL-6R, and sgp130 levels. Blood collected from the heart of mice during sacrifice was used for the measurement of human sIL-6, sIL-6R, and sgp130. Concentrations of sIL-6, sIL-6R, and sgp130 were determined using ELISA procedures.[17] Microtiter 96-well plates were coated with 2.5 μg/ml anti-human IL-6 (Cat.# IM-R109, Diaclone Research), 2.5 μg/ml anti-human IL-6R (Cat.# MAB227, R & D Systems), and 2.5 μg/ml anti-human gp130 (Cat.# 42228, Genzyme-Techne) for 2 h at 37°C followed by washing 3 times with PBS containing 0.1% Tween 20. The plates were blocked with 3% BSA at 37°C for 2 h and washed 3 times with the same washing buffer. sIL-6, sIL-6R, and sgp130 standards and unknown samples were added and incubated at 37°C for 2 h, and then the plates were washed. To detect bound sIL-6, sIL-6R, and sgp130, biotinylated anti-human IL-6 (50 ng/ml, Cat.# 44206, Genzyme-Techne), IL-6R (50 ng/ml, Cat.# 44227, Genzyme-Techne), and gp130 (50 ng/ml, Cat.# 44228, Genzyme-Techne) was added and the plates were incubated for 2 h at 37°C, followed by washing. Horseradish peroxidase-conjugated streptavidin was added and incubation was continued at 37°C for 30 min, followed by washing 3 times with washing buffer. Peroxidase activity was determined using TMB as a substrate. The reaction was stopped with 1.8 *M* H_2SO_4, and the absorbance was measured at 450 nm.

Electrophoresis mobility shift assay (EMSA). Nuclear extracts were prepared as described previously.[15] Nuclear extracts (5 μg of protein) were incubated in 12 μl of binding buffer (10 mmol/liter HEPES, pH 7.8, 100 mmol/liter NaCl, 1 mmol/liter EDTA, 2.5% glycerol), 1 μg of poly [d(I-C)] and ^{32}P-labeled κB probe derived from the H-2K promoter for 30 min at room temperature. To identify the subunits constituting the NF-κB complexes, specific Abs against p50, c-Rel (Santa Cruz Biotechnology), p65 (#1226), RelB (#13482) (from Dr. Nancy Rice), and p52 (#1319) (from Upstate Biotechnology) were used. Antibody was added to the nuclear extract, and the mixture was allowed to stand for 30 min at room temperature before incubation with the radiolabeled probe. DNA-protein complexes were analyzed by electrophoresis in 5% polyacrylamide gel in 0.5× TBE (44.5 mmol/liter Tris, 44.5 mmol/liter boric acid, 1 mmol/liter EDTA). After electrophoresis, the gels were dried and subjected to autoradiography.

Results

Efficient engraftment and rapid tumor formation of MM cells in NOG mice without change of histomorphology or tumor marker expression. To investigate the *in vivo* growth, MM cell lines [KMM-1 and U-266] were inoculated either s.c. in the post-auricular region or i.v. in the tail of NOG mice (Table 1). Mice inoculated s.c. with cell line KMM-1 produced a visible tumor

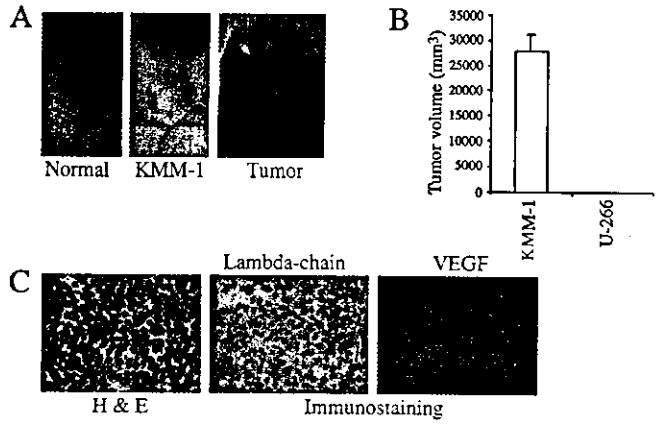

Fig. 1. Growth and tumor marker expression of multiple myeloma KMM-1 cells in NOG mice. A: Photograph of a normal mouse (left panel), a mouse inoculated with KMM-1 cells s.c. in the post-auricular region after 40 days (middle panel), and a s.c. KMM-1 tumor 40 days after inoculation of cells (right panel). B: s.c. tumor growth of mice inoculated with KMM-1 cells, shown as the mean±SEM from 19 mice. C: H&E and immunohistochemical staining of tumor tissue of KMM-1 cell-inoculated mice. The left panel represents H&E staining. Immunohistochemical staining was conducted using anti-human λ-chain (middle panel) and VEGF antibodies (right panel).

Table 1. *In vivo* **growth of multiple myeloma cell lines in NOG mice**

Cell lines	No. of cells inoculated per mouse[1]	Inoculation route[2]	Day of sacrifice after inoculation	No. of mice with tumor/ no. of mice inoculated[3]
KMM-1	10×10^6	s.c.	40	19/19
KMM-1	2×10^6	i.v.	40	3/3
U-266	10×10^6	s.c.	60	0/3
U-266	2×10^6	i.v.	60	0/3

1) Mice were inoculated with 2×10^6 to 10×10^6 cells per mouse.
2) s.c., subcutaneous; i.v., intravenous.
3) Number of animals in which tumor developed.

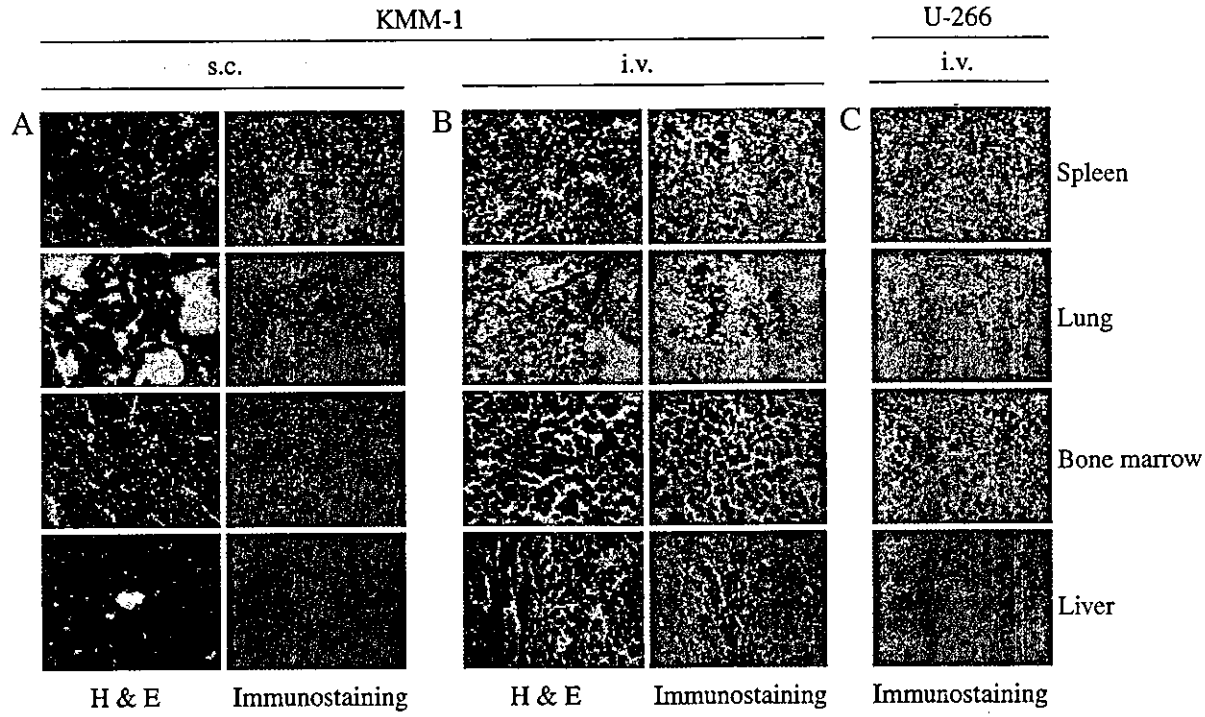

Fig. 2. Infiltration of MM cells in various organs of NOG mice. A and B: H&E and immunohistochemical staining of spleen, lung, bone marrow, and liver of mice injected with KMM-1 cells either s.c. or i.v. C: Immunohistochemical staining of spleen, lung, bone marrow, and liver of mice i.v.-injected with U-266 cells. Left and right panels of figure A and B represent H&E and immunostaining, respectively. Immunohistochemical staining was conducted using anti-human λ-chain antibody.

within 2 weeks in NOG mice while i.v.-inoculated mice were found to have a solid tumor in the peritoneal cavity after sacrifice. The KMM-1 cell line was most efficient in the formation of a large tumor (Fig. 1A), as well as development of severe anemia and clinical signs of near-death, such as piloerection, weight loss, and cachexia, in NOG mice at the time point of sacrifice, while U-266 was ineffective. The average tumor size (mean=27,893 mm^3) in NOG mice inoculated s.c. with KMM-1 was determined 40 days after inoculation (Fig. 1B). To test whether tumors maintain the original histomorphology and expression patterns of tumor markers in NOG, we performed H&E and immunostaining of tumor tissues obtained from mice inoculated with KMM-1 cells. Histological and immunological analysis revealed that *in vivo* tumor cells retained their morphology well, and expressed human λ Ig light chain and VEGF. These results showed that MM cell line-inoculated NOG mice generated large tumors very efficiently. This extremely rapid tumor formation in all mice without change of histomorphology or tumor marker expression is one of the hallmarks of our animal model.

Infiltration of MM cells into various organs of NOG mice. To assess the tissue distribution of MM cells, we carried out histological examinations of various organs of NOG mice after inoculation of the cells. Proliferation and infiltration of tumor cells were found not only in primary tumor tissues, but also in peripheral blood and to a lesser extent in spleen and lung of NOG mice inoculated s.c. with the KMM-1 cell line (Fig. 2A). We found that KMM-1 cells exhibited infiltration in spleen, lung, liver, and bone marrow of mice after i.v. inoculation (Fig. 2B), while U-266 cells did so to a lesser degree only in bone marrow (Fig. 2C). H&E and immunohistochemical staining showed a degree of infiltration of tumor cells at the site of inoculation and in various organs with KMM-1 and U-266 (Fig. 2, A, B, and C). These data suggest that MM cell line could invade different organs of NOG mice in a similar manner to myeloma cells in patients. Interestingly, MM cells appeared to

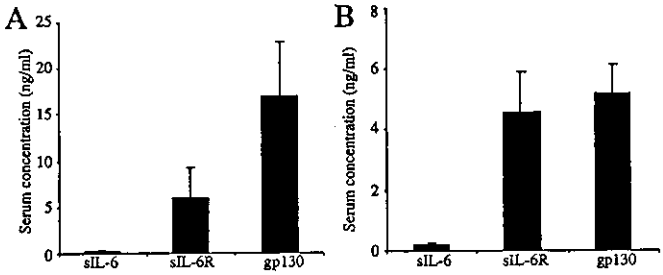

Fig. 3. Serum levels of sIL-6, sIL-6R, and sgp130 in NOG mice inoculated with KMM-1 cells, determined by ELISA. A and B: Data obtained from mice inoculated s.c. (12 mice) and i.v. (3 mice) with KMM-1 cells, respectively.

infiltrate various organs of mice more aggressively and massively after i.v. inoculation than after s.c. inoculation.

Serum soluble human IL-6R and gp130 levels as indicators of MM cell proliferation in NOG mice. Numerous studies have established that sIL-6R levels are significantly elevated in serum from MM patients.[18-21] MM cell uptake in SCID mice was associated with the presence of circulating sIL-6R and sgp130.[22] Serum human IL-6, IL-6R, and gp130 levels measured 40 days after inoculation of MM cells. sIL-6R [mean=6.42 ng/ml (s.c.) and 4.57 ng/ml (i.v.)] and sgp130 [mean=16.13 ng/ml (s.c.) and 5.17 ng/ml (i.v.)], but not IL-6, were markedly elevated in mice that were found to be successfully engrafted with KMM-1 cells (Fig. 3, A and B). Mice inoculated with U-266 cells showed no increase in serum sIL-6R or sgp130 (data not shown), even though histological analysis of bone marrow showed some infiltration of U-266 cells after i.v. inoculation (Fig. 2C).

NF-κB binding activity of KMM-1 cells inoculated in NOG mice. High NF-κB binding activity is thought to be crucial for maintaining the characteristics of MM cells in patients.[23,24] To determine whether or not NF-κB activity is changed *in vivo*, we

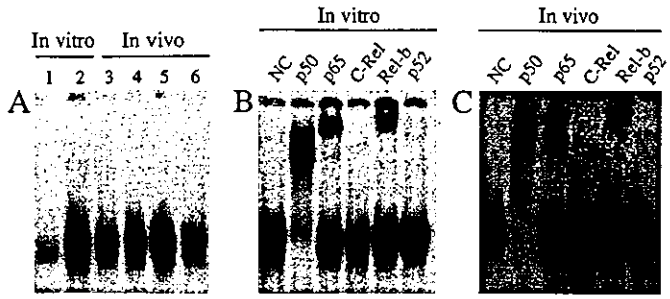

Fig. 4. Unaltered NF-κB binding activity of KMM-1 cells in NOG mice. A: Analysis by EMSA of NF-κB binding activity of the KMM-1 cells derived from cells cultured *in vitro* or tumor cells. Nuclear extracts (5 μg) were treated with ^{32}P-labeled wild-type NF-κB oligonucleotides. Lane 1 contains the negative control using Jurkat, and lane 2 contains *in vitro*-cultured KMM-1 cells. Lanes 3 to 6 show *in vivo* NF-κB DNA binding of KMM-1 cells from four different tumor-bearing mice. B and C: Analysis of NF-κB components of KMM-1 cells by super-shift assay. Super-shift using antibodies specific to p50, p65, c-Rel, RelB, and p52 subunits of NF-κB was conducted for both *in vitro* (B) and *in vivo* (C) samples. NC, negative control.

performed EMSA (Fig. 4A). Tumor cells from mice retained a strong NF-κB DNA binding activity, similar to that *in vitro*. We also investigated the DNA binding of NF-κB components in tumor cells in comparison with that of cells cultured *in vitro*. For this purpose, super-shift assays were performed with nuclear extracts of tumor tissues in the absence or presence of Abs that specifically recognize the following members of the NF-κB family: p50, p65, c-Rel, RelB, and p52. The results indicated that the induced NF-κB complexes contained p50, p65, and RelB both *in vitro* and *in vivo* in the case of KMM-1 (Fig. 4, B and C, respectively). These results also suggested that NF-κB activity is required for MM cell growth in NOG mice, and could be a therapeutic target for myeloma.

Discussion

Recent advances in the studies of MM have suggested new avenues for treatment and potential cure of this disease. To achieve these goals, it is essential to establish an effective animal model. Although several models, mainly using conventional SCID mice, are available, there are many problems. Representative data for the establishment of animal models for MM are as follows. a) By 3 months after inoculation of MM cell lines, a distinct solid tumor was formed at the inoculated site in one of five mice and re-transplantation was indispensable.[5] b) Mice were given whole-body irradiation followed by inoculation of MM cells.[6,7] c) When fetal bones were implanted in SCID mice to provide a human microenvironment, human MM cells grew in these bones.[8,9] d) Intraperitoneal tumors were observed in only 50% of animals when the mice received anti-gp130 mAbs.[10,22] The differences in behavior of MM cell lines in different types of SCID mice as regards the formation of tumors are dependent on the host immune system; natural killer cells might play an important role in the rejection of implanted tissues or cells in SCID mice.[25-28] In addition, recipient dendritic cells could have a role in transplant rejection.[29] In addition to the absence of T- and B-cells, NOG mice have no NK and there are functional defects in dendritic cells.[16] In the present study, MM cells inoculated s.c. in the post-auricular region over the skeleton of mice permitted us to quickly observe the tumor growth macroscopically and to measure the size of the tumor. By measuring the size of the tumor macroscopically, it was possible to easily compare the growth ability of inoculated tumor cells between the controls and mice treated with drugs or other agents. It is noteworthy that MM cells were found to infiltrate various organs of mice more aggressively and massively after i.v. inoculation than after s.c. administration. Indeed, circulating levels of sIL-6R may act as a useful prognostic marker, since high serum sIL-6R concentrations were associated with death of patients within 3 years of diagnosis.[19] Our results indicate that the presence of high levels of human sIL-6R and sgp130 in mouse serum is linked to development of tumor growth and clinical signs of imminent death. The implantation procedure is easily performed, the engraftment is highly efficient and expression levels of tumor markers, NF-κB activity and components are not altered. The present animal and inoculation system should be applicable to other malignant cells and cell lines of different origins that are unrelated to MM (unpublished results), and could be very useful in the study of tumorigenesis in general.

In summary, the reproducible growth behavior and preservation of characteristic features of MM cells suggest that our NOG mouse model can provide a unique opportunity to investigate the mechanisms of pathogenesis and malignant cell growth of myeloma, and to develop novel therapeutic regimens.

We thank S. Ichinose of Instrumental Analysis Research Center, Shu Endo of the Animal Research Center, Tokyo Medical and Dental University, and Peter J. Richard of Cardiff University, Wales, UK for their advice and assistance with the experiments. we also thank Y. Sato of the National Institute of Infectious Diseases for her skillful technical assistance. This work was supported by grants from the Ministry of Education, Culture, Sports, Science and Technology and Ministry of Health, Labour and Welfare of Japan.

1. Hallek M, Bergsagel PL, Anderson KC. Multiple myeloma: increasing evidence for a multistep transformation process. *Blood* 1998; **91**: 3–21.
2. Aguayo A, Estey E, Kantarjian H, Mansouri T, Gidel C, Keating M, Giles F, Estrov Z, Barlogie B, Albitar M. Cellullar vascular endothelial growth factor is a predictor of outcome in patients with acute myeloid leukemia. *Blood* 1999; **94**: 3717–21.
3. Carmeliet P, Jain RK. Angiogenesis in cancer and other diseases. *Nature* 2000; **407**: 249–57.
4. Bataille R, Manolagas SC, Berenson JR. Pathogenesis and management of bone lesions in multiple myeloma. *Hematol Oncol Clin North Am* 1997; **11**: 349–361.
5. Uneda S, Hata H, Matsuno F, Nagasaki A, Harada N, Mitsuya Y, Matsuzaki H, Mitsuya H. A nitric oxide synthase inhibitor, N^G-nitro-L-arginine methyl ester, exerts potent antiangiogenic effects on plasmacytoma in a newly established multiple myeloma severe combined immunodeficienct mouse model. *Br J Haematol* 2003; **120**: 396–404.
6. Dingli D, Timm M, Russell SJ, Witzig TE, Rajkumar SV. Promising preclinical activity of 2-methoxyestradiol in multiple myeloma. *Clin Cancer Res* 2002; **8**: 3948–54.
7. Miyakawa Y, Ohnishi Y, Tomisawa M, Monnai M, Kohmura K, Ueyama Y, Ito M, Ikeda Y, Kizaki M, Nakamura M. Establishment of a new model of human multiple myeloma using NOD/SCID/γc^{null} (NOG) mice. *Biochem Biophys Res Commun* 2004; **313**: 258–62.
8. Yaccoby S, Barlogie B, Epstein J. Primary myeloma cells growing in SCID-hu mice: a model for studying the biology and treatment of myeloma and its manifestations. *Blood* 1998; **92**: 2908–13.
9. Yaccoby S, Epstein J. The proliferative potential of myeloma plasma cells manifest in the SCID-hu host. *Blood* 1999; **94**: 3576–82.
10. Reme T, Gueydon E, Jacquet C, Klein B, Brochier J. Growth and immortalization of human myeloma cells in immunodeficient severe combined immunodeficient mice: a preclinical model. *Br J Haematol* 2001; **114**: 406–13.
11. Quarmby S, Kumar S, Kumar P. Radiation-induced normal tissue injury: role of adhesion molecules in leukocyte-endothelial cell interactions. *Int J Cancer* 1999; **82**: 385–95.
12. Adam L, Crepin M, Lelong J, Spanakis E, Israel L. Selective interactions between mammary epithelial cells and fibroblasts in co-culture. *Int J Cancer* 1994; **59**: 262–8.
13. Sawhney N, Garrahan N, Douglas-Jones A, Williams ED. Epithelial stomal interaction in tumors. *Cancer* 1992; **70**: 2115–20.

14. Van Roosendaal C, Van Ooijen B, Klijn JG, Claassen L, Eggemont AM, Henzen-Logmans SC, Foehens JA. Stromal influences on breast cancer cell growth. *Br J Cancer* 1992; **65**: 77–81.
15. Dewan MZ, Terashima K, Teruishi M, Hasegawa H, ItoM, Tanaka Y, Mori N, Sata T, Koyanagi Y, Maeda M, Kubuki Y, Okayama A, Fujji M, Yamamoto N. Rapid tumor formation of HTLV-1-infected cell lines in novel NOD-SCID/γc^{null} mice: suppression by an inhibitor against NF-κB. *J Virol* 2003; **77**: 5286–94.
16. Ito M, Hiramatsu H, Kobayashi K, Suzue K, Kawahata M, Hioki K, Ueyama Y, Koyanagi Y, Sugamura K, Tsuji K, Heike T, Nakahata T. NOD/SCID/γc^{null} mouse: an excellent recipient mouse model for engraftment of human cells. *Blood* 2002; **100**: 3175–82.
17. Jones SA, Novick D, Horiuchi S, Yamamoto N, Szalai A, Filler GM. C-Reactive protein: a physiological activation of interleukin 6 receptor shedding. *J Exp Med* 1999; **189**: 599–604.
18. Ohtani K, Niomiya H, Hasegawa Y, Kobayashi T, Kojima H, Nagasawa T, Abe T. Clinical significance of elevated soluble interleukin-6 receptor levels in the sera of patients with plasma cell dyscrasias. *Br J Haematol* 1995; **91**: 116–20.
19. Pulkki K, Pelliniemi T-T, Rajamaki A, Tienhaara A, Laakso M, Lahtinen R. Soluble interleukin-6 receptor as a prognostic factor in multiple myeloma. *Br J Haematol* 1995; **92**: 370–4.
20. Kyrtsonis M, Dedoussis G, Zervas C, Perifanis V, Baxevanis C, Stamatelon M, Maniatis A. Soluble interleukin-6 receptor (sIL-6R), a new prognostic factor in multiple myeloma. *Br J Haematol* 1996; **93**: 398–400.
21. Kyriakou D, Papadaki H, Eliopoulos AG, Foudoulakis A, Alexandrakis M, Eliopoulos GD. Serum soluble IL-6 receptor concentrations correlate with stages of multiple myeloma defined by serum beta 2-microglobulin and C-reactive protein. *Int J Haematol* 1996; **66**: 367–71.
22. Rebouissiou C, Wijdenes J, Autissier P, Tarte K, Costes V, Liautard J, Rossi J-F, Brochier J, Klein B. A gp130 interleukin-6 transducer-dependent SCID model of human multiple myeloma. *Blood* 1998; **91**: 4727–37.
23. Landowski TH, Olashaw NE, Agrawal D, Dalton WS. Cell adhesion-mediated drug resistance (CAM-DR) is associated with activation of NF-kappa B (BelB/p50) in myeloma cells. *Oncogene* 2003; **22**: 2417–21.
24. Hideshima T, Chauhan D, Richardson P, Mitsiades C, Mitsiades N, Hayashi T, Munshi N, Dong L, Castro A, Palombella V, Adams J, Anderson KC. NF-κB as a therapeutic target in multiple myeloma. *J Biol Chem* 2002; **277**: 16639–47.
25. Feuer G, Stewart SA, Baird SM, Lee F, Feuer R, Chen ISY. Potential role of natural killer cells in controlling tumorigenesis by human T-cell leukemia viruses. *J Virol* 1994; **69**: 1328–33.
26. Dorshkind K, Pollack SB, Bosma MJ, Phillips RA. Natural killer (NK) cells present in mice with severe combined immunodeficiency (scid). *J Immunol* 1985; **134**: 3798–801.
27. Bukowshi JF, Warner JF, Dennert G, Welsh RM. Adoptive transfer studies demonstrating the antiviral effect of natural killer cells *in vivo*. *J Exp Med* 1985; **161**: 40–52.
28. Welsh RM. Regulation of virus infections by natural killer cells: a review. *Nat Immun Cell Growth Regul* 1986; **5**: 169–99.
29. Lechler R, Ng WF, Steinman RM. Dendritic cells in transplantation-friends or foe? *Immunity* 2001; **14**: 357–68.

JOURNAL OF VIROLOGY, Sept. 2004, p. 9842–9853
0022-538X/04/$08.00+0 DOI: 10.1128/JVI.78.18.9842–9853.2004

Vol. 78, No. 18

A Consecutive Priming-Boosting Vaccination of Mice with Simian Immunodeficiency Virus (SIV) *gag/pol* DNA and Recombinant Vaccinia Virus Strain DIs Elicits Effective Anti-SIV Immunity

Kenji Someya,[1,2] Ke-Qin Xin,[2] Kazuhiro Matsuo,[1] Kenji Okuda,[2] Naoki Yamamoto,[1] and Mitsuo Honda[1]*

AIDS Research Center, National Institute of Infectious Diseases, Toyama, Shinjuku-ku, Tokyo,[1] and Department of Bacteriology, Yokohama City University, School of Medicine, Fukuura, Kanazawa-ku, Yokohama,[2] Japan

Received 8 August 2003/Accepted 18 May 2004

To evaluate immunity induced by a novel DNA prime-boost regimen, we constructed a DNA plasmid encoding the *gag* and *pol* genes from simian immunodeficiency virus (SIV) (SIV*gag/pol* DNA), in addition to a replication-deficient vaccinia virus strain DIs recombinant expressing SIV *gag* and *pol* genes (rDIsSIV*gag/pol*). In mice, priming with SIV*gag/pol* DNA, followed by rDIsSIV*gag/pol* induced an SIV-specific lymphoproliferative response that was mediated by a $CD4^+$-T-lymphocyte subset. Immunization with either vaccine alone was insufficient to induce high levels of proliferation or Th1 responses in the animals. The prime-boost regimen also induced SIV Gag-specific cellular responses based on gamma interferon secretion, as well as cytotoxic-T-lymphocyte responses. Thus, the regimen of DNA priming and recombinant DIs boosting induced Th1-type cell-mediated immunity, which was associated with resistance to viral challenge with wild-type vaccinia virus expressing SIV*gag/pol*, suggesting that this new regimen may hold promise as a safe and effective vaccine against human immunodeficiency virus type 1.

As human immunodeficiency virus type 1 (HIV-1) continues to spread throughout the world (16, 27, 51, 42), the need for a safe and effective prophylactic vaccine is more urgent now than ever (16, 27, 43, 51). A realistic goal for such a vaccine is to limit HIV-1 infection by eliciting immune responses that reduce the viral load and prevent disease progression. With other viral diseases, T-helper-cell type 1 (Th1)-mediated immune responses and $CD8^+$ cytotoxic T lymphocytes (CTL) have been reported to provide protection and reduce disease progression (11, 17, 23, 34, 45, 55, 77). Moreover, Th1/$CD8^+$ T-cell responses have been shown to play an important role in controlling HIV-1 replication (9, 28, 41, 44, 50, 52, 56, 60, 61, 62). In previous studies, nonhuman primates and chimpanzees immunized with attenuated strains of simian immunodeficiency virus (SIV) or HIV-1 had strong antigen-specific immune responses and were protected from challenge with SIV, simian/human immunodeficiency virus (SHIV), or HIV-1 (1, 15, 66, 81). These studies demonstrate that an experimental immunogen is capable of mediating protection against intravenous and mucosal viral challenge in animal models of HIV and SIV, although attenuated HIV-1 vaccines are generally considered to be unsafe for use in humans (4, 21).

Recently, HIV-1 DNA-based vaccines have been shown to induce protective T-cell-mediated immune responses (12, 13, 33, 57, 75). To increase vaccine efficacy, DNA has also been modified by codon optimization, as well as by coinjection with cytokine-encoding plasmids, recombinant proteins, and other vaccine vectors (7, 10, 29, 32, 46). The immune response to DNA vaccines based on HIV-1 antigen genes was increased when innate and adaptive cytokine genes were combined (5, 14, 22). Furthermore, enhanced levels of protection were demonstrated with a combination regimen consisting of DNA priming (SIV *gag*, *pol*, *vif*, *vpx*, and *vpr*, and HIV-1 *env*, *tat*, and *rev*), followed by boosting with a recombinant modified vaccinia virus Ankara (MVA)-based vaccine (SIV*gag* and *pol* and HIV-1 *env*) (2).

Recombinant MVA has been used frequently as a booster vaccine in various combination regimens. In an effort to develop additional safe booster antigens, we generated a recombinant vaccine based on the vaccinia virus strain DIs, which has proven not to replicate in all mammalian cells tested (25). The virologic and immunologic properties of the DIs vector have been reported previously by our group (25, 26, 38, 70, 71). The vaccinia virus DIs vector expressing SIV Gag protein elicited immune responses able to suppress SHIV infection in macaques (26). In the present study, we have demonstrated enhanced Th1-type immune induction in mice primed with a plasmid DNA vaccine encoding SIV*gag/pol*, followed by boosting with a newly developed recombinant DIs strain that expresses SIV*gag/pol* (rDIsSIV*gag/pol*). Our result demonstrates that this new prime-boost regimen is both safe and effective at eliciting anti-immunodeficiency viral immunity, suggesting its promise as a potential vaccine against HIV-1.

MATERIALS AND METHODS

Animals. Female BALB/c mice ($H\text{-}2^d$) were obtained from Shizuoka Laboratory Center (Shizuoka, Japan) and were used at between 8 and 12 weeks of age.

Construction of SIV*gag/pol* encoding plasmid DNA. Plasmid DNA encoding SIV*gag/pol* was prepared by standard procedures as previously described (47, 48, 64). Briefly, SIV*gag/pol* DNA was derived from the eucaryotic expression vector pcDNA3.1(−) (Invitrogen, Carlsbad, Calif.). pcDNA3.1(−) was digested with XhoI and EcoRI and ligated to SIV*gag* and *pol* genes that were amplified from SHIV-C2/1 DNA (GenBank no. AF217181) with the primers 5′-AACTCGAG

* Corresponding author. Mailing address: AIDS Research Center, National Institute of Infectious Diseases, 1-23-1 Toyama, Shinjuku-ku, Tokyo 162-8640, Japan. Phone: 81-3-5285-1111, ext. 2737. Fax: 81-3-5285-1183. E-mail: address: mhonda@nih.go.jp.

AAGATAGAGTGGGAGATGGG and AAGAATTCAGGCTATGCCACCT CTCTA-3′. *gag/pol* genes were derived from the molecular clone SIV_{mac239}. The correct insertion of SIV*gag/pol* DNA into the plasmid was confirmed by PCR.

Generation and propagation of rDIsSIV*gag/pol*. rDIsSIV*gag/pol* was constructed based on the previously described protocol (25, 26). The SIV*gag/pol* gene was first amplified from $SHIV_{NM-3rN}$ DNA (24) by using primers SGP-5 (5′-AATACCCGGGATGGGCGTGAGAAACTC) and SGP-3 (AATAGAGC TCCTATGCCACCTCTCTAG-3′) and then subcloned into the pUCvvp7.5H vector (25, 26). A HindIII fragment encoding SIV*gag/pol* and the p7.5H promoter region were inserted into the HindIII site of a pUC/DIs transfer vector. rDIsSIV*gag/pol* and a control vector expressing the gene for LacZ (rDIsLacZ) were generated by homologous recombination and propagated in chicken embryo fibroblasts (CEF). Each virion preparation was purified by sucrose density ultracentrifugation and stored at −120°C. The expression of a 55-kDa protein corresponding to SIV Gag was confirmed by Western blotting with extracts from CEF infected with rDIsSIV*gag/pol* and anti-SIV Gag-specific monoclonal antibodies (IB6 or V10) (35).

SIV antigens. Overlapping 15-mer peptides spanning SIV Gag (with 11-amino-acid overlaps) were provided from the NIH AIDS Research and Reference Reagent Program (National Institutes of Health, Rockville, Md.). Peptides spanning Gag p27 and p15 regions were divided into eight pools and used as antigens. Purified native SIV p27 Gag protein (SIV Gag) was purchased from Advanced Biotechnologies, Inc. (Rockville, Mass.).

Lymphocyte proliferative assays. Lymphocyte proliferative assays were performed as previously described (19). One week after the final vaccination, the mice in each of five groups (see Fig. 2) were sacrificed. The spleens were removed, and the tissue was disrupted by compression through a cell strainer (Becton Dickinson, Franklin Lakes, N.J.). Isolated spleen cells were pooled and resuspended at 10^6 cells/ml in RPMI 1640 medium supplemented with 10% fetal bovine serum, L-glutamine, penicillin, and streptomycin. The $CD4^+$-T-cell, $CD8^+$-T-cell, or $CD4^+/CD8^+$-T-cell fraction was then depleted by using magnetic cell sorting (MACS; Miltenyi Biotech, Bergisch Gladbach, Germany) (20, 63). Aliquots of cells (100 μl) were transferred to 96-well round-bottom plates in triplicate. Either 1 μg of native purified SIV p27 Gag protein or pooled peptides (1 μg/peptide/10^5 cells) per ml was added to each well. The cells were incubated at 37°C in 5% CO_2 for 2 days before the addition of 1 μCi of [^{3}H]thymidine. After an additional 24 h of incubation, the cells were harvested, and the uptake of ^{3}H was determined. The results are expressed as the stimulation index (SI), which was calculated as a ratio of the counts per minute in the presence or absence of antigen.

Analysis of antigen-specific cytokine production. To further characterize the type of immune response induced in the vaccinated mice, $CD4^+$ T cells were isolated from the total spleen cell population by using MACS as described above. The purity of the isolated $CD4^+$ T cells was determined by flow cytometric analysis to be >98% (20, 63). The purified $CD4^+$ T cells were cultured for 3 days at a density of 10^6 cells/ml in the presence of pooled peptides or SIV Gag protein at a concentration of 10 μg/ml, along with T-cell-depleted and irradiated feeder cells at a density of 10^6 cells/ml. Culture supernatants were collected, and the concentrations of gamma interferon (IFN-γ), interleukin-2 (IL-2), IL-4, IL-5, IL-6, and IL-10 were measured by using commercially available enzyme-linked immunosorbent assay (ELISA) kits (Amersham, Arlington Heights, Ill.).

IFN-γ-specific ELISPOT assays. SIV-specific IFN-γ-producing cells were enumerated by using an enzyme-linked immunospot assay (ELISPOT) and a murine IFN-γ ELISPOT kit (Diaclone Research, Besacon, France). Aliquots (100 μl) of cell suspensions containing 10^5 spleen cells were transferred to 96-well plates that were coated with anti-mouse IFN-γ antibody. Then, 1 μg of either SIV Gag protein or pooled peptides (1 μg/peptide/10^5 cells) was added, and the plates were incubated for 24 h at 37°C in 5% CO_2. The plates were then washed three times and incubated with biotinylated anti-mouse IFN-γ antibody for 1 h at 37°C. IFN-γ-specific cells were detected by using streptavidin-alkaline phosphatase conjugate and BCIP (5-bromo-4-chloro-3-indolylphosphate) substrate (Roche, Mannheim, Germany). Wells were imaged, and spot-forming cells (SFC) were counted by using a KS ELISPOT compact system (Carl Zeiss, Oberkochen, Germany). An SFC was defined as a large black spot with a fuzzy border (40). To determine significance levels, a baseline for each peptide pool was established by using the average and standard deviation (SD) of the number of SFC for each peptide. A threshold significance value, which corresponded to this average plus two SDs, was then determined. A response was considered positive if the number of SFC exceeded the threshold significance level of the control wells with no added peptide.

SIV Gag-specific CTL assays. Lymphocytes from the vaccinated mice were evaluated for CTL activity by using ^{51}Cr release assays as previously described by Takahashi et al. (72). In brief, spleen cells removed from red blood cells were resuspended in RPMI 1640 medium supplemented with 10% fetal bovine serum, L-glutamine, 2-mercaptoethanol, penicillin, and streptomycin. The cell suspensions containing 10^7 spleen cells were restimulated with 0.1 μg/peptide/10^7 cells of pooled peptides for 5 days. IL-2 containing rat T-cell-stimulated culture supernatant (T-STIM; Collaborative Res. Bedford, Mass.) was added 3 days after cell culture. Cells from the *H-2*^{d} haplotype line, M12.4.5, were used as targets. M12.4.5 cells were incubated with $Na_2^{51}CrO_4$ (3.7 MBq/10^7 cells) for 90 min at 37°C in 5% CO_2 before being pulsed with peptides (either 40 or 50 μg). After 1 h, the target cells were thoroughly washed with RPMI 1640 and then dispensed into 96-well V-bottom plates (10^4 cells/well). The in vitro-stimulated effector cells were added, and the plates were incubated for 4 h at 37°C. To determine the spontaneous or maximum release of ^{51}Cr, target cells were incubated with medium alone or treated with 2% Triton X-100, respectively. The percent specific lysis was calculated by using the following formula: (experimental release − spontaneous release)/(maximum release − spontaneous release).

SIV Gag-specific humoral responses. SIV Gag-specific antibody endpoint titer was measured by ELISA as previously described (67). ELISA plates were coated with 0.3 μg of SIV Gag protein (Advanced Biotechnologies) per well. Heat-inactivated pooled mice sera were serially diluted and then added to the ELISA plates. Gag-specific antibody bound to Gag protein was captured with alkaline phosphatase-labeled goat anti-mouse immunoglobulin G (Southern Biotechnology Associates, Inc., Birmingham, Ala.).

Evaluation of vaccine-induced immunity by virus challenge. To address whether the immune responses induced by the vaccination were protective, mice were challenged with wild-type vaccinia virus recombinant expressing SIV*gag/pol* (vv9019; National Institute for Biological Standards and Control, Blanch Lane, Hertfordshire, United Kingdom). The viral challenge was performed by using the method set forth by Belyakov et al. (8) and Qiu et al. (54). At 6 days after final vaccination, four mice in each vaccinated group and four naive mice were intraperitoneally (i.p.) challenged with 10^7 PFU of vv9019. One week after the challenge with the recombinant vaccinia virus expressing SIV*gag/pol*, the mice were sacrificed, and their ovaries were removed. The ovaries were homogenized, sonicated, and assayed for the challenge virus titer by plating serial 10-fold dilutions on a plate of CEF. After 3 days of culture, the plates were stained with 0.2% of crystal violet, and plaque were counted at each dilution. The results were expressed as the fold of the reduction in vaccinia virus titer in vaccinated mice versus the titer in naive mice.

ELISPOT assay for gag, pol, or whole vaccinia virus antigen-specific immunity. The magnitude of T-cell responses against SIV Gag, Pol, and vaccinia virus antigens was also measured by ELISPOT assay based on the recombinant vaccinia virus stimulation method described previously (74, 80). Briefly, spleen cells isolated from normal mouse were infected with 10 PFU per cell of either SIV gag-expressing wild-type vaccinia virus (vvSIV gag; National Institute for Biological Standards and Control), SIV pol-expressing wild-type vaccinia virus (vvSIV pol; National Institute for Biological Standards and Control), or nonrecombinant wild-type vaccinia virus (Vaccinia WR; National Institutes of Health) for 16 h and then fixed with paraformaldehyde. The virus antigen-expressing cells were used as stimulator cells and cultured with spleen cells of vaccinated mice at a stimulator/responder ratio of 1:2, and each antigen-specific ELISPOT assay was performed by the method described above.

Statistical analysis. Data are expressed as the mean ± the SD, and data analysis was carried out by using the StatView program (SAS Institute, Cary, N.C.). A P value of <0.05 was considered significant. The comparative analysis of animal groups subjected to different vaccine regimens was performed by using the Kruskal-Wallis H-test, followed by the Student-Newman-Keul correction.

RESULTS

Construction and expression of SIV*gag/pol* DNA and rDIsSIV*gag/pol*. The *gag/pol* region of SIV_{mac239} was inserted into two selected vectors. The first, pcDNA3.1(−), a eukaryotic expression vector, was used as the backbone of the SIV*gag/pol* DNA vaccine (Fig. 1A), and the second, pUC/DIs, was used as a transfer vector to generate rDIsSIV*gag/pol* and the control vector, rDIsLacZ (Fig. 1B). PCR was used to confirm that the SIV*gag/pol* DNA had been correctly inserted into each vector and Gag-specific Western blots were used

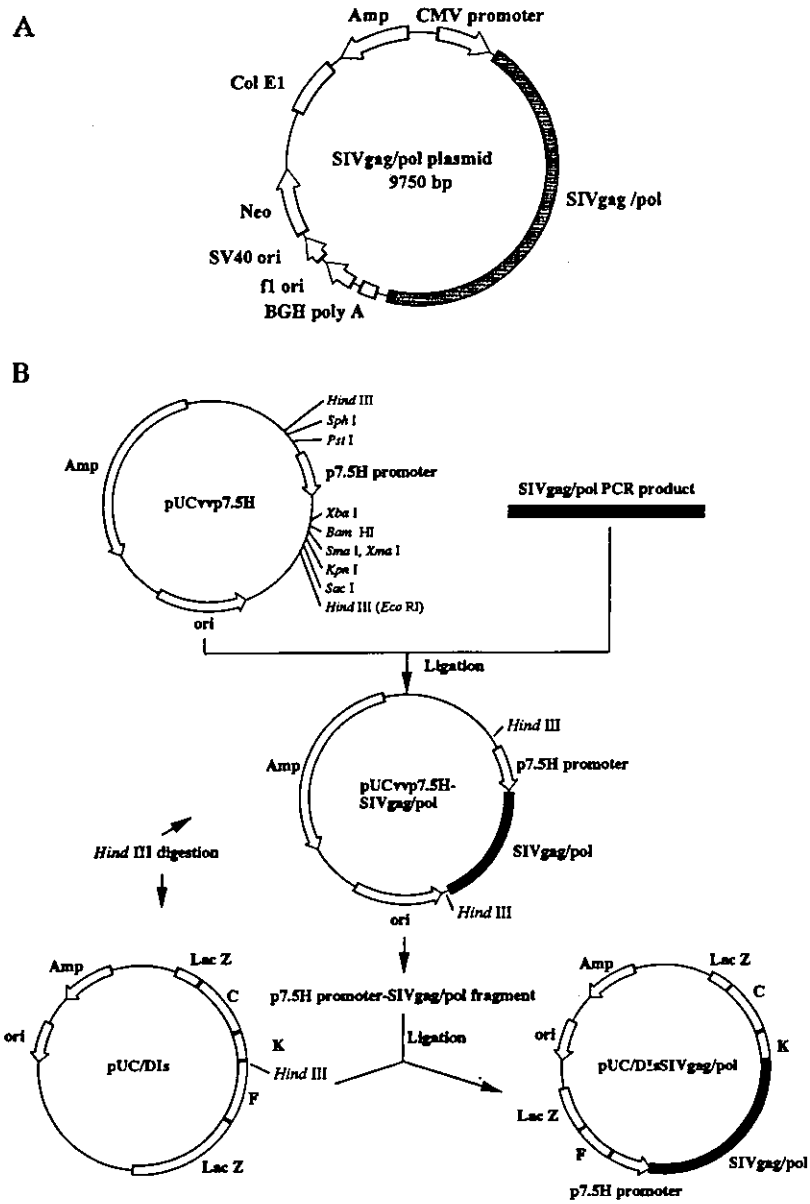

FIG. 1. Construction of SIV*gag/pol* expression vectors. (A) SIV*gag/pol* plasmid DNA; (B) construction and generation of recombinant DIsSIV*gag/pol*. The ampicillin resistance gene and vaccinia virus early/late promoter p7.5H are designated by Amp and p7.5H, respectively. Arrows indicate the direction of transcription. Hatched and white blocks represent the SIV*gag/pol* gene and HindIII fragments of vaccinia virus DNA, respectively.

to verify in vitro expression of the SIV Gag protein (data not shown).

Prime-boost regimen. A total of 50 BALB/c mice were divided into five groups of 10 mice each. Group 1 received three intramuscular injections (50 μg of each) of SIV*gag/pol* DNA at 2-week intervals, followed by two injections of rDIsLacZ (10^6 PFU each) at with 1-week intervals. Similarly, group 2 mice received three injections with 50 μg of control DNA pcDNA3.1 (−), followed by two injections of rDIsLacZ (10^6 PFU each) at 1-week intervals. Group 3 received three 50-μg intramuscular injections of SIV*gag/pol* DNA; 4 weeks later, the mice in group 3 were boosted with two intradermal injections of rDIsSIV*gag/pol* (10^6 PFU each) with a 1-week interval. The mice in group 4 received three injections of control DNA (50 μg of each), followed by two injections of rDIsSIV*gag/pol* (10^6 PFU each) (Fig. 2). In group 5, mice were immunized with SIV*gag/pol* DNA five times at the same intervals as described above. We confirmed the original data by the second run of the experiments with 50 additional animals and statistically summarized the challenge results (see Fig. 9).

The prime-boost vaccine regimen generates antigen-specific $CD4^+$-T-lymphocyte proliferative responses. SIV Gag-specific T-lymphocyte proliferative responses were measured in splenocytes from immunized mice with either SIV Gag protein or peptides spanning the full-length Gag protein of SIV_{mac239}. Spleen cells from mice in groups 1, 3, 4, and 5 showed signif-

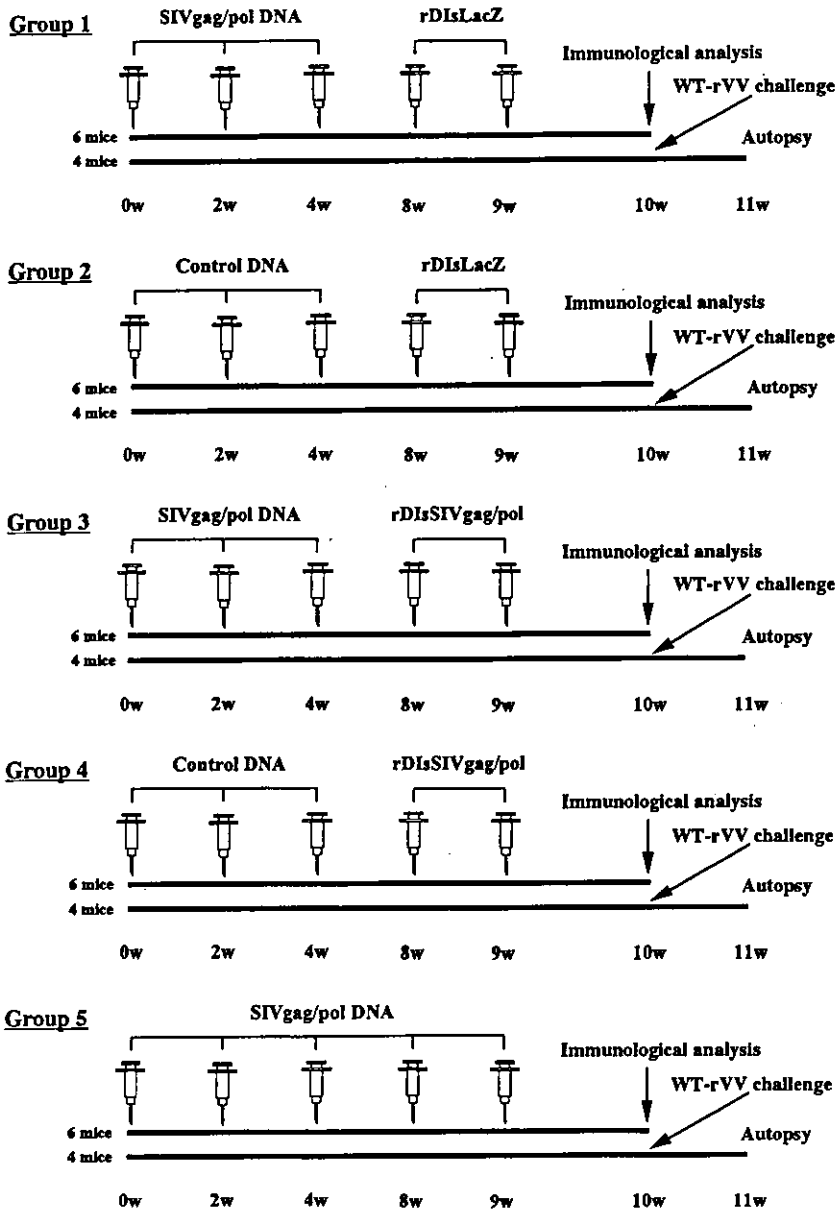

FIG. 2. Schematic of the experimental protocol for immunization and viral challenge. BALB/c mice were divided into five groups of 10 mice each (groups 1 to 5) and immunized three times consecutively with SIV*gag/pol* DNA and then twice with rDIsLacZ (group 1), three times with control DNA and then twice with rDIsLacZ (group 2), three times with SIV*gag/pol* DNA and then twice with rDIsSIV*gag/pol* (group 3), three times with control DNA and then twice with rDIsSIV*gag/pol* (group 4), or five times with SIV*gag/pol* DNA (group 5).

icant levels of proliferation in response to stimulation with SIV Gag protein and peptide pools (Fig. 3), whereas no proliferative activity (SI < 3) was seen with splenocytes from control group 2. Among the five animal groups, splenocytes from the mice in group 3 (immunized with a prime-boost regimen) showed the highest levels of T-cell proliferative responses against SIV Gag proteins ($P < 0.01$). The mean SIs for each of the five groups were 3.6 ± 1.2, 0.8 ± 0.4, 9.3 ± 2.3, 4.4 ± 1.5, and 3.4 ± 0.96, respectively (SIV Gag protein-stimulated group in Fig. 3A). Depletion of the $CD4^+$- or $CD4^+$ $CD8^+$-T-cell fraction from group 3's splenocytes dramatically reduced the proliferative responses to <10% (Fig. 3B). In contrast, the proliferative activity was not affected by the depletion of the $CD8^+$ fraction from the cell suspensions.

The splenocytes from the mice in group 3 also exhibited the highest proliferative responses against pooled peptides spanning the full-length SIV Gag protein (Fig. 3). Among the three positive peptide pools (4, 6, and 7), reactivity to pool 6 was the highest, with a mean SI of 5.4 ± 2.8 (Fig. 3A). Peptides in this pool correspond to the SIV p27 region and encode an SIV-specific $CD4^+$-T-cell epitope, which is recognized by the $H\text{-}2^d$ allele. Splenocytes from mice in control group 2 were not reactive with any of the SIV antigens (SI < 1.0).

Immunization with the prime-boost regimen induces Gag-specific Th1-type responses. To further characterize the type

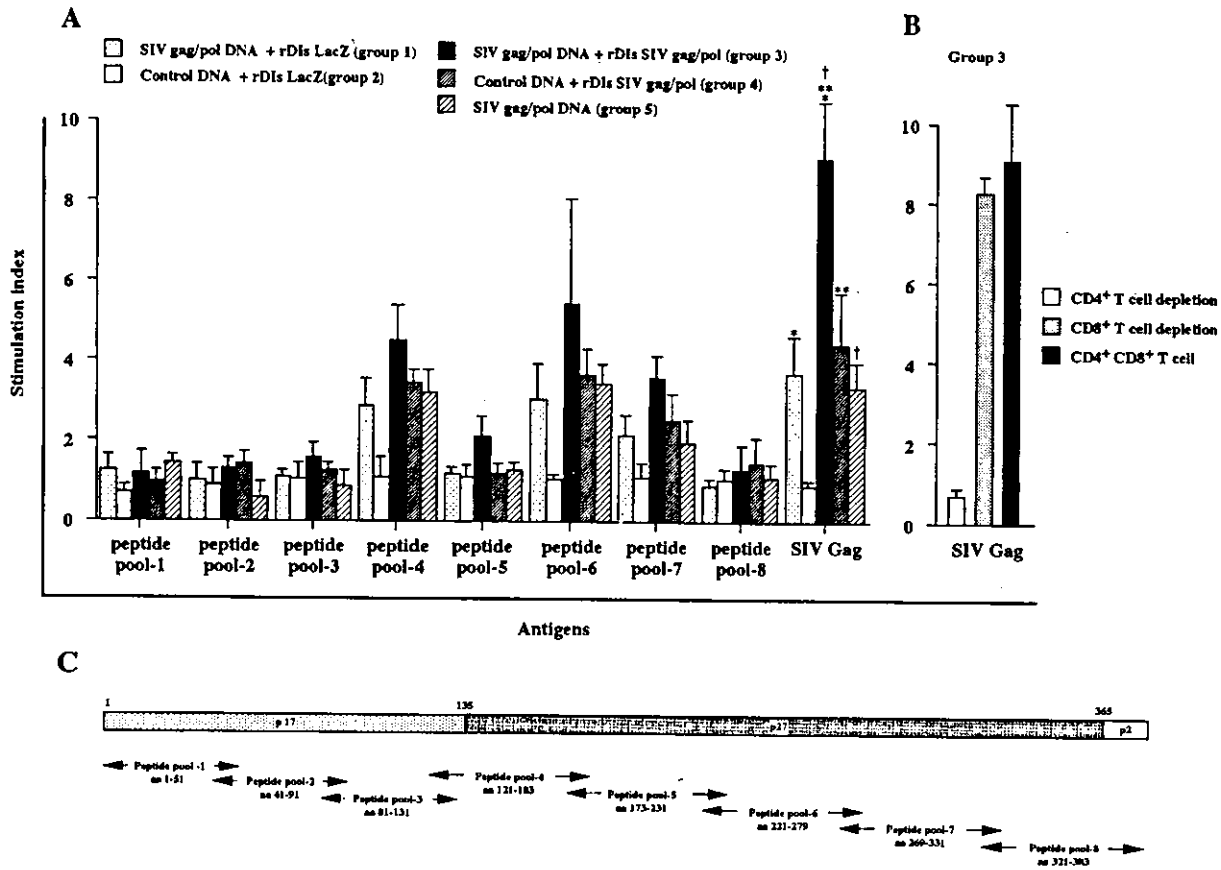

FIG. 3. Induction of SIV Gag-specific lymphocyte proliferative responses. (A) Spleen cells were cultured in the presence or absence of SIV Gag antigens, and [^{3}H]thymidine incorporation was measured as described in Materials and Methods. Proliferative responses are expressed as the SI. (B) Aliquots of spleen cells from mice vaccinated with the prime-boost regimen were depleted of either the CD4$^+$-T-cell, the CD8$^+$-T-cell, or the CD4$^+$ CD8$^+$-T-cell subpopulation prior to measuring SIV Gag-specific proliferative responses (C). Set of 15-mer overlapping peptides spanning the full-length Gag protein of SIV_{mac239}. The peptides were grouped into eight pools to evaluate cell-mediated immune responses. Values indicated by the single asterisk, double asterisks, and dagger symbol all showed a P value of <0.01, which were compared to give the indicated P values between groups 1 and 3, groups 3 and 4, and groups 3 and 5, respectively.

of immune responses induced by a prime-boost vaccination with SIV*gag/pol* DNA and rDIsSIV*gag/pol*, efforts were made to identify distinct antigen-specific CD4$^+$-T-helper-cell subsets. CD4$^+$ T cells were isolated from splenocytes and restimulated in vitro with purified SIV Gag protein. Culture supernatants were then examined for evidence of antigen-specific Th1- or Th2-type cytokine secretion. CD4$^+$ T cells from the immunized mice in group 3 (prime-boost regimen) generated the highest levels of Th1 cytokines, including IFN-γ and IL-2, whereas no evidence was found for the secretion of Th2 cytokines such as IL-4, IL-5, IL-6, or IL-10 (Fig. 4). The levels of cytokines generated by CD4$^+$ T cells from mice belonging to control group 2 were undetectable. These results demonstrate that priming with SIV*gag/pol* DNA, followed by boosting with rDIsSIV*gag/pol*, effectively induces predominantly Th1-type cytokine production in mice.

Characteristics of SIV-specific immunities in immunized animals at virus challenge. The induction of antigen-specific IFN-γ secretion and CTL was also evaluated in the immunized mice. ELISPOT assays were used to measure the number of SIV-specific SFC secreting IFN-γ in splenocytes from the immunized mice in each group (Fig. 5). Cells were restimulated in vitro with either SIV Gag p27 protein or pooled peptides spanning the full-length SIV Gag. SIV Gag-specific SFC were induced in mice receiving SIV*gag/pol* DNA alone, rDIsSIV*gag/pol* alone, or the combined prime-boost regimen. The number of SFC was higher in spleen cells from mice of group 3 immunized with the prime-boost regimen when stimulated with SIV Gag p27 than with Gag protein (735 ± 124 SFC per 10^6 splenocytes) than in those of mice immunized with either SIV*gag/pol* DNA or rDIsSIV*gag/pol* alone ($P < 0.01$). Stimulation of spleen cells of group 3 with whole Gag showed a stronger response than with Gag peptide pools 3, 5, and 8, with ELISPOT activities of 582 ± 121, 532 ± 117, and 394 ± 85 SFC per 10^6 splenocytes, respectively.

To determine whether the prime-boost regimen was able to induce antigen-specific CTL, ^{51}Cr-release assays were performed 1 week after the final inoculation. Spleen cells were isolated and restimulated in vitro for 7 days with each of eight different peptide pools. Cytotoxic activity was evaluated at effector/target (E:T) ratios of 100:1 to 12.5:1. SIV Gag-specific CTL activity was detected after stimulation with peptide pools 3, 5, and 8 (Fig. 6). The highest specific activity was induced by the prime-boost regimen after restimulation with peptide pool

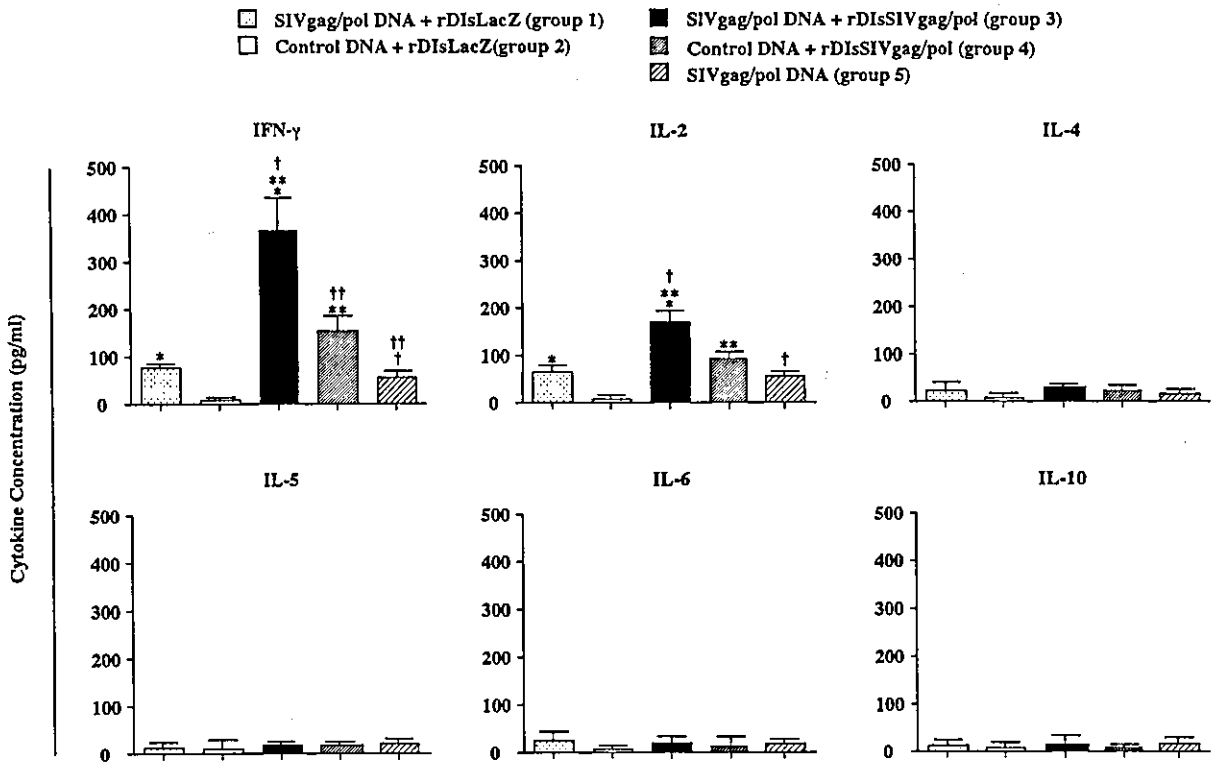

FIG. 4. In vitro production of IFN-γ, IL-2, IL-4, IL-5, IL-6, and IL-10 from spleen cells of immunized mice. Spleen cells were stimulated with recombinant SIV Gag protein, and secreted cytokines were quantified by cytokine-specific ELISA. The single asterisk, double asterisks, and dagger symbol all indicate a P value of <0.01, and the double dagger symbol (‡) indicates a P value <0.05, compared to give the indicated P values between groups 1 and 3, groups 3 and 4, groups 3 and 5, and groups 4 and 5, respectively.

3 (60% ± 11% specific lysis at an E:T ratio of 100:1). In contrast, spleen cells restimulated with peptides from pools 1, 2, 4, 6, and 7 showed little (<20%) or no specific lysis, as did cells from animals vaccinated with control DNA. CTL activity induction paralleled that of IFN-γ-secreting SFC (Fig. 5) and was dependent on the choice of immunizing and restimulating antigens.

We studied whether this regimen also enhances specific antibody responses (Fig. 7). Three consecutive inoculations of SIV*gag/pol* DNA, followed by two of rDIsLacZ in group 1 and five consecutive SIV*gag/pol* DNA vaccinations in group 5, showed low levels of Gag-specific antibody responses, with ELISA titers of <120 throughout the immunization period. Group 4 animals receiving three control DNAs, followed by two rDIsSIV*gag/pol* vaccinations, and group 5 animals with the prime-boost vaccination also elicited low levels of SIV Gag-specific antibody responses with titers of <180, showing that the induction of SIV Gag-specific humoral responses are very low in these vaccination regimens.

Elicitation of positive immunity by the prime-boost vaccine regimen against challenge with the wild-type SIV*gag/pol*-expressing vaccinia virus. Seven days after final vaccination, immunized mice were challenged i.p. with 10^7 PFU of the wild-type vaccinia virus strain vv9019, which expressed SIV*gag/pol*. At 6 days after the viral challenge, the mice were sacrificed, and ovaries were harvested to determine the viral load of the challenge virus in the organs. Among the five vaccinated groups, group 3 mice immunized by the prime-boost vaccine regimen showed a striking inhibition of viral infection into ovaries, with a fold reduction as high as 322 ± 48 (dark column in Fig. 8). The mice immunized with other regimens of group 1, 2, 4, or 5 (Fig. 2) showed fold reductions of 52 ± 23, 4 ± 5, 112 ± 21, and 41 ± 10, respectively, in the virus titer. By comparing the different groups with each other and with naive mice, we defined that the prime-boost vaccine group 3 showed statistically the most significant reduction of the viral load of the wild-type virus in tissues ($P < 0.01$). However, although vaccinated with SIV*gag/pol* prime and rDIsSIV*gag/pol* boost, group 3 exhibited no protection when challenged with wild-type vaccinia virus. The comparable vaccine efficacy to these animal groups were achieved by a second-series immunization experiment with 50 more animals (Fig. 9). These results suggest that vaccination with an SIV*gag/pol* DNA prime, followed by a rDIsSIV*gag/pol* boost, leads to a protective immunity against challenge with wild-type recombinant vaccinia virus in the immunized animals.

Gag-specific responses dominate in the positive immunity induced by the prime-boost regimen at the time of challenge. We then studied the immune responses by differentiating the gag-, pol-, and vaccinia virus antigen-specific responses in respective antigen-specific ELISPOT assays (Fig. 10). At the time of vv9019 challenge, we defined not only SIV Gag- but also SIV Pol-specific T-cell responses in immunized animals in groups 1, 3, 4 and 5. However, the Gag response was remarkably higher than the Pol response in group 3 of the prime-boost regimen ($P < 0.01$) with a less pronounced but similar ten-

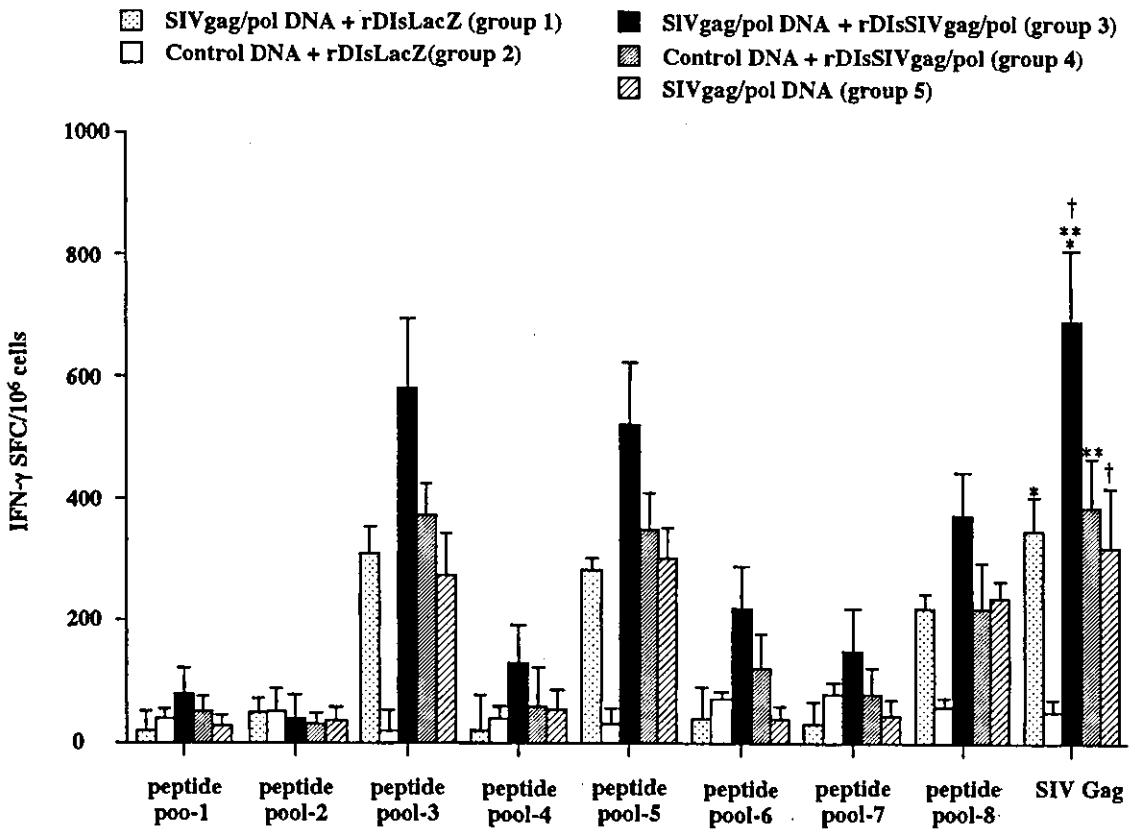

FIG. 5. Frequency of SIV Gag-specific IFN-γ-producing cells in immunized mice. Spleen cells were stimulated with either SIV Gag protein or pooled SIV Gag peptides. IFN-γ-producing cells were detected by IFN-γ-specific ELISPOT assays, and data are expressed as the number of SFC per 10^6 splenocytes. The single asterisk, double asterisks, and dagger symbol all showed a P value of <0.01, which were compared to give the indicated P values between groups 1 and 3, groups 3 and 4, and groups 3 and 5, respectively.

dency seen in groups 1, 4, and 5 ($P < 0.01$). In contrast, vaccinia virus antigen-specific ELISPOT activities were all extremely low, and the positive spots numbered fewer than 80 per million of spleen cells among vaccinia virus- and recombinant vaccinia virus-inoculated groups 2, 3, and 4. The results were not significantly different among the three groups of animals tested, suggesting that the very low levels of vaccinia virus antigen-specific immunity do not significantly contribute to the induction of positive immunity in the prime-boost regimen. These findings demonstrate that the SIVGag-specific T-cell responses dominate in the elicitation of positive immunity induced by the prime-boost vaccine regimen with vaccines expressing SIV*gag/pol*.

DISCUSSION

Previously, we demonstrated that DNA-based vaccination results in the induction of virus-specific immunity to several viral pathogens, including HIV-1 (3, 47, 48, 53, 64, 76). Furthermore, we recently established a system to express HIV-1 genes by inserting them into a deleted region of the attenuated vaccinia virus strain, DIs (25, 30, 71). Like the parental DIs strain, the recombinant DIs-HIV was shown to be completely replication deficient in mammalian cells. Moreover, the expression of SIVGag was sufficient to elicit positive immunity against pathogenic viral challenge in a SHIV-macaque model (26). In the present study, the prime-boost regimen with HIV-DNA and rDIs-HIV clearly enhanced the protective efficacy over that of rDIs-HIV alone or HIV-DNA alone. Although it is not possible to directly compare protective efficacy among different vector-based vaccine models, recombinant vaccinia virus strains (including MVA) (69), a substrain of Copenhagen (NYVAC) (73), and recombinant adenovirus-HIV strains (68), our results appear to be as effective for obtaining protective immunity as those achieved with vector-based vaccines. Taken together, these results suggest that a combination regimen of DNA and rDIs might be used as a safe and effective vaccine.

In the present study, we addressed whether a prime-boost regimen consisting of a plasmid DNA prime and rDIs boost could promote a strong Th1-type immune response capable of affecting the outcome of experimental challenge. It has been proposed that Th1-type responses are associated with protection against infection, including HIV-1 infection and AIDS. Individuals who control HIV-1 viremia in the absence of antiviral therapy respond to HIV-1 Gag protein and its helper epitopes with a Th1-like response, producing IFN-γ and β-chemokines (58). Moreover, a shift from Th1- to Th2-dominant cytokine production occurs during the course of HIV-1 disease progression (36, 39, 65), suggesting that the cytokine profile may be indicative of a T helper phenotype and represent a

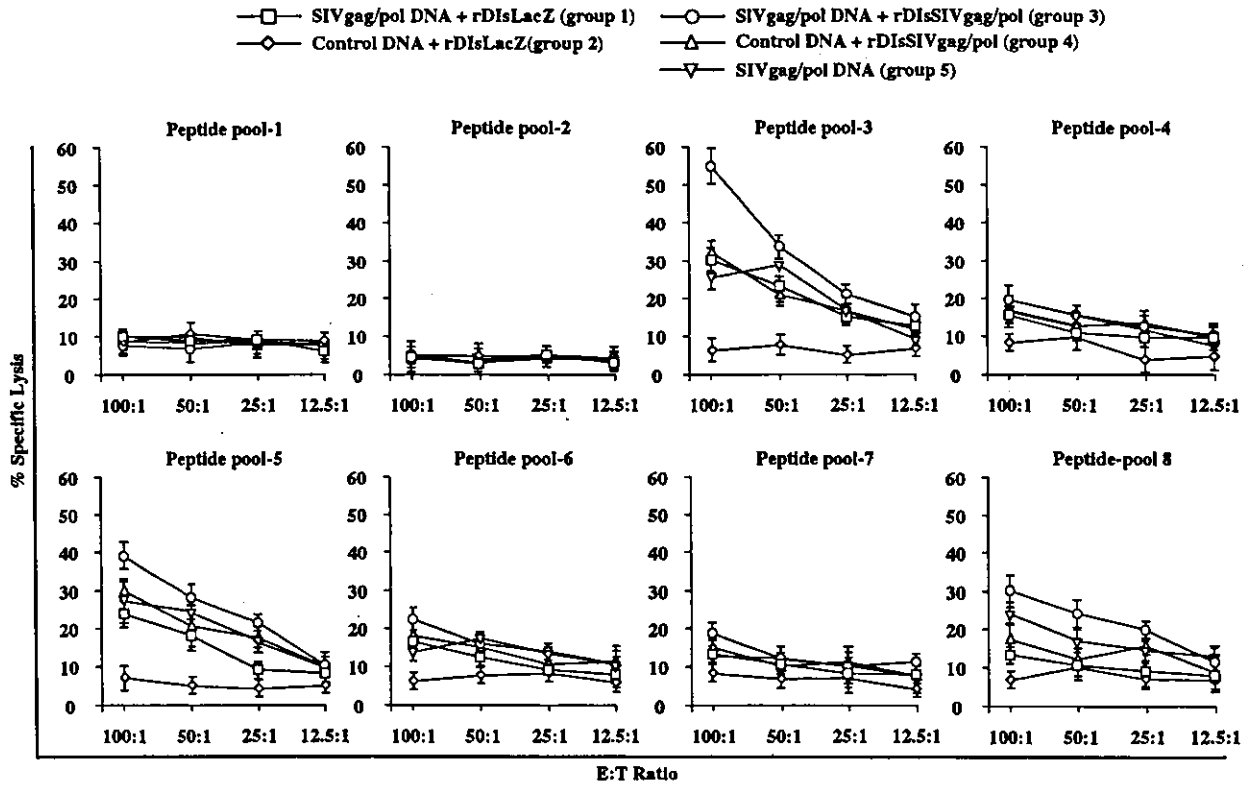

FIG. 6. Induction of SIV Gag-specific CTL in immunized mice. Spleen cells were stimulated with pooled SIV Gag peptides and tested in ^{51}Cr release assays with peptide pulsed M12.4.4 cells as targets cells at E:T ratios ranging from 100:1 to 12.5:1.

response to infection. Our results demonstrate that Th1-type cytokines, including IL-2 and IFN-γ, are secreted by $CD4^+$ T cells from mice immunized with a prime-boost regimen targeting the SIV*gag/pol* region. These Th1-type responses were associated with SIV Gag protein- or peptide-specific SFC activity

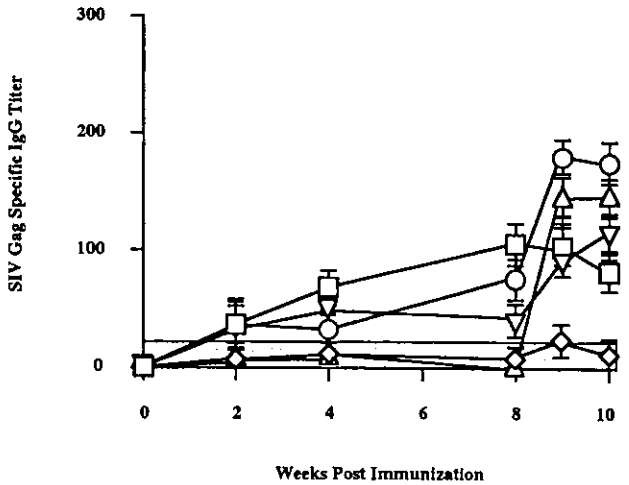

FIG. 7. Kinetics of binding antibody titer specific for SIV Gag in mice. The endpoint titers of immune sera were measured by the SIV Gag p27 antigen-ELISA at each time point. Bars represent the mean ± the SD value of four independent experiments. Symbols: □, SIV*gag/pol* DNA + rDIsLacZ (group 1); ◇, control DNA + rDIsLacZ (group 2); ○, SIV*gag/pol* DNA + rDIsSIV*gag/pol* (group 3); △, control DNA + rDIsSIV*gag/pol* (group 4); ▽, SIV*gag/pol* DNA (group 5).

and $CD8^+$ CTL. These observations are encouraging in light of the hypothesis that Th1-mediated immunity is associated with resistance to HIV infection and virus suppression (6, 31). In vitro restimulation of splenocytes from mice immunized with the prime-boost regimen generated high levels of Th1 cytokines, such as IL-2 (>100 pg/ml) and IFN-γ (>300 pg/ml), and lower levels of Th2 cytokines, such as IL-4, IL-5, IL-6, and IL-10 (<30 pg/ml). In contrast, immunization with either SIV*gag/pol* DNA or rDIsSIV*gag/pol* alone led to lower levels of Th1-type cytokine production, suggesting that the prime-boost regimen is superior for the induction of SIV Gag-specific Th1-type T-cell responses.

Having observed an induction of SIV Gag-specific Th1-type responses in mice after immunization with the prime-boost regimen, we also detected significant levels of virus-specific proliferative responses in spleen cells from the immunized animals. Fractionation of the spleen cell population revealed that the SIV-specific lymphocyte responses were mediated by $CD4^+$ T cells. Several reports have demonstrated that HIV-1-specific $CD4^+$ T-cell proliferation inversely correlates with disease progression in infected individuals (37, 78). Moreover, HIV-1 Gag p24-specific $CD4^+$-lymphocyte proliferation has been shown to be inversely correlated with the HIV-1 load in plasma (58, 59). Although SIV-specific T-cell proliferative responses were induced in mice immunized with either SIV*gag/pol* DNA or rDIsSIV*gag/pol* alone, the SI was generally not as high as that obtained by the combined prime-boost regimen. Our data showing the induction of $CD4^+$-T-cell proliferative responses to SIV Gag in mice immunized with the

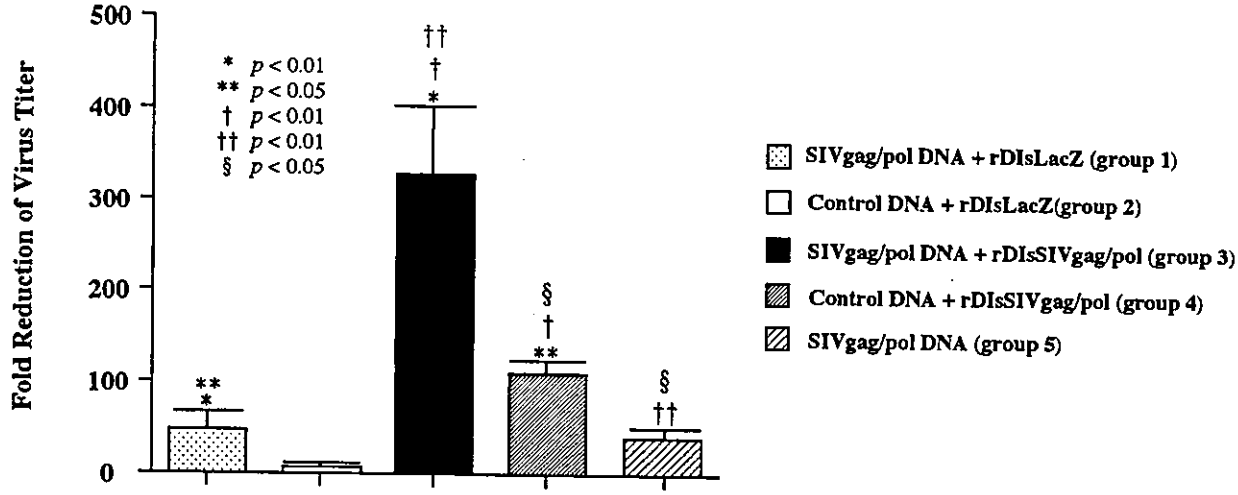

FIG. 8. The prime-boost vaccine regimen augmented protective immune responses. The animals immunized with five different strategies were challenged i.p. with 10^7 PFU of wild-type vaccinia virus strain vv9019 recombinant expressing SIV*gag/pol*. The bar shows the fold reduction of vaccinia virus titer in the ovaries of vaccinated mice versus naive mice. Bars show the geometric mean values of four mice per group.

prime-boost regimen suggests this vaccine approach may be effective at inducing strong virus-specific $CD4^+$-T-cell responses capable of controlling viral load in the immunized animals.

The importance of T helper responses is highlighted in reports that antigen-specific $CD4^+$ T helper cells may promote CTL activity either by a CD4-antigen-presenting cell-CD8 pathway and IL-2 secretion (18, 58, 79) or by an increased production of antiviral cytokines and chemokines. Furthermore, $CD4^+$ T cells promote other types of cell-mediated immunity, including activation of macrophages and cytokine secretion, which may also contribute to the control of HIV-1 and other intracellular pathogens. Recent reports have documented that a vaccine regimen consisting of a DNA prime and a recombinant poxvirus boost generates pathogen-specific protective immune responses (2). The protective role of CTL is also well documented in HIV-1 infection (9, 28, 41, 44, 50, 52, 56, 60, 61, 62), and the induction of an HIV-1-specific CTL population is considered an important goal for most current vaccine strategies. HIV-1 Gag-specific $CD8^+$ cytolysis has been highly correlated with IFN-γ synthesis by $CD8^+$ spleen T cells (49). In the present study, the prime-boost regimen induced significant levels of SIV Gag-specific IFN-γ-producing cells (>700 SFC/10^6 splenocytes). These responses were higher than those induced by immunization with either SIV*gag/pol* DNA or rDIsSIV*gag/pol* alone.

In conclusion, our data show that a new vaccine regimen consisting of SIV*gag/pol* DNA priming and rDIsSIV*gag/pol* boosting induces strong SIV Gag-specific and Th1-type cellular immune responses, which were associated with the control of viral challenge. Since the magnitude and phenotype of the induced immunity are believed to be associated with protection against viral infection and disease progression, this new priming-boosting vaccine regimen may be useful for the develop-

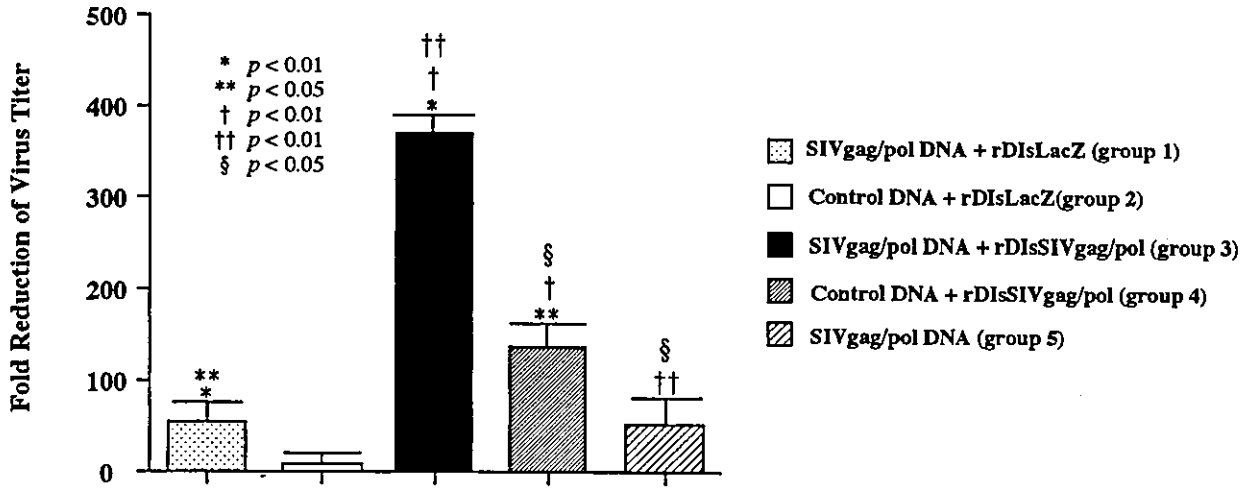

FIG. 9. A second series immunization with the prime-boost regimen resulted in a similar augmentation of protective immune responses. Fifty animals were divided into five groups of 10 animals each, and the animales were immunized by the five different strategies, respectively, described in Fig. 8.